

UNIVERSITY OF CALIFORNIA

Santa Barbara

**Mathematical Approaches to Understanding Mammalian  
Circadian Rhythms**

by

**Peter C. St. John**

Committee in charge:

Professor Francis J. Doyle III, Chair

Professor Samir Mitragotri

Professor Michelle A. O'Malley

Professor Linda R. Petzold

June 2015

The dissertation of Peter C. St. John is approved.

---

SAMIR MITRAGOTRI

---

DATE

---

MICHELLE A. O'MALLEY

---

DATE

---

LINDA R. PETZOLD

---

DATE

---

FRANCIS J. DOYLE III, COMMITTEE CHAIR

---

DATE

Mathematical Approaches to Understanding Mammalian Circadian Rhythms

Copyright ©2015

by

Peter C. St. John

# Acknowledgement

Hello, here is some text without a meaning. This text should show what a printed text will look like at this place. If you read this text, you will get no information. Really? Is there no information? Is there a difference between this text and some nonsense like “Huardest gefburn”? Kjift – not at all! A blind text like this gives you information about the selected font, how the letters are written and an impression of the look. This text should contain all letters of the alphabet and it should be written in of the original language. There is no need for special content, but the length of words should match the language.

This is the second paragraph. Hello, here is some text without a meaning. This text should show what a printed text will look like at this place. If you read this text, you will get no information. Really? Is there no information? Is there a difference between this text and some nonsense like “Huardest gefburn”? Kjift – not at all! A blind text like this gives you information about the selected font, how the letters are written and an impression of the look. This text should contain all letters of the alphabet and it should be written in of the original language. There is no need for special content, but the length of words should match the language.

And after the second paragraph follows the third paragraph. Hello, here is some text without a meaning. This text should show what a printed text will look like at this place. If you read this text, you will get no information. Really? Is there no information? Is there a difference between this text and some nonsense like “Huardest

## *Acknowledgement*

---

gefburn”? Kjift – not at all! A blind text like this gives you information about the selected font, how the letters are written and an impression of the look. This text should contain all letters of the alphabet and it should be written in of the original language. There is no need for special content, but the length of words should match the language.

After this fourth paragraph, we start a new paragraph sequence. Hello, here is some text without a meaning. This text should show what a printed text will look like at this place. If you read this text, you will get no information. Really? Is there no information? Is there a difference between this text and some nonsense like “Huardest gefburn”? Kjift – not at all! A blind text like this gives you information about the selected font, how the letters are written and an impression of the look. This text should contain all letters of the alphabet and it should be written in of the original language. There is no need for special content, but the length of words should match the language.

Hello, here is some text without a meaning. This text should show what a printed text will look like at this place. If you read this text, you will get no information. Really? Is there no information? Is there a difference between this text and some nonsense like “Huardest gefburn”? Kjift – not at all! A blind text like this gives you information about the selected font, how the letters are written and an impression of the look. This text should contain all letters of the alphabet and it should be written in of the original language. There is no need for special content, but the length of words should match the language.

# Vita of Peter C. St. John

## Contact Information

Department of Chemical Engineering  
University of California, Santa Barbara  
Santa Barbara, CA 93106-5080

*Phone:* (508) 494-2474  
*E-mail:* [pstjohn@engineering.ucsb.edu](mailto:pstjohn@engineering.ucsb.edu)  
*Office:* Engineering II, Rm. 1508

## Education

**University of California, Santa Barbara**  
*Ph.D. Candidate, Department of Chemical Engineering*

**September 2010 - present**  
Santa Barbara, California

**Tufts University**  
*BS, Chemical and Biological Engineering*

**September 2006 - May 2010**  
Medford, Massachusetts

## Honors and Awards

CAST Student Travel Grant	<b>September 2014</b>
Society for Research on Biological Rhythms (SRBR) Research Merit Award	<b>June 2014</b>
Best Poster, Center for Chronobiology Symposium, UCSD	<b>February 2014</b>
1 <sup>st</sup> Place, SRBR Logo Competition	<b>January 2014</b>
Mitsubishi Chemical Fellowship Recipient	<b>2012-2015</b>
UCSB Scienceline 2011-2012 Life Science Outstanding Answerer	<b>June 2012</b>
National Science Foundation GRFP Honorable Mention	<b>April 2011</b>
Class of 1947 Victor Prather Prize	<b>May 2010</b>
Max Tischler Prize Scholarship	<b>May 2009</b>
Elected to Tau Beta Pi	<b>September 2008</b>

## Publications

**St. John, P.C.**, Taylor, S.R., Abel, J.H., and F.J. Doyle III. Amplitude metrics for cellular circadian bioluminescence reporters (2014) *Biophysical Journal*, 107 (11) pp. 2712-2722

**St. John, P.C.**, Hirota, T., Kay, S.A. and F.J. Doyle III. Spatiotemporal separation of PER and CRY posttranslational regulation in the mammalian circadian clock (2014) *PNAS*, 111 (5) pp. 2040-2045.

Yang, R., Rodriguez-Fernandez, M., **St. John, P.C.**, and F.J. Doyle III. Chapter 8 – Systems Biology (2014) In E. Carson and C. Cobelli (Eds.) *Modelling Methodology for Physiology and Medicine, 2nd Edition*, pp. 159-187.

**St. John, P.C.**, and F.J. Doyle III. Estimating confidence intervals in predicted responses for oscillatory biological models (2013) *BMC Systems Biology* 7:71.

Hirota, T., Lee, J.W., **St. John, P.C.**, Sawa, M., Iwaisako, K., Noguchi, T., Pongsawakul, P.Y., Sonntag, T., Welsh, D.K., Brenner, D.A., Doyle, F.J. III, Schultz, P.G., Kay, S.A., Identification of small molecule activators of cryptochrome (2012) *Science*, 337 (6098) pp. 1094-1097.

Murphy A.R., **St. John P.C.**, Kaplan D.L. Modification of silk fibroin using diazonium coupling chemistry and the effects on hMSC proliferation and differentiation (2008) *Biomaterials*, 29 (19), pp. 2829-2838.

## Contributed Talks

**St. John, P.C.**, and F.J. Doyle III. November 2014. Development of Amplitude Response Curves for Single-Cell and Population-Level Circadian Systems. *To be presented at the 2014 AIChE Annual Meeting, Atlanta, GA*

**St. John, P.C.**, and F.J. Doyle III. June 2014. Amplitude metrics for uncoupled cellular circadian bioluminescence reporters. Presented at the Society for Research on Biological Rhythms Meeting, Big Sky, MT.

**St. John, P.C.**, and F.J. Doyle III. October 2012. Cryptochrome balancing for period control: mathematical insights into circadian clock design. Presented at the Model-based Analysis and Control of Cellular Processes Workshop, Purdue University, West Lafayette, IN.

## Poster Presentations

**St. John, P.C.**, and F.J. Doyle III. February 2014. Spatiotemporal separation of PER and CRY post-translation regulation. Presented at the UCSD Center for Chronobiology Symposium, La Jolla, CA.

**St. John, P.C.**, T. Hirota, S.A. Kay, and F.J. Doyle III. July 2013. Estimating confidence intervals in model predictions to determine plausible mechanisms for small molecule modifiers. Presented at the Chronobiology Gordon Research Conference, Newport, RI.

**St. John, P.C.**, and F.J. Doyle III. February 2013. Predictive confidence intervals from mathematical circadian models. Presented at the UCSD Center for Chronobiology Symposium, La Jolla, CA.

**St. John, P.C.**, T. Hirota, S. Kay, and F.J. Doyle III. May 2012. Cryptochrome balancing for period control. Presented at the Meeting of the Society for Research on Biological Rhythms, Destin, FL.

**St. John, P.C.**, and F.J. Doyle III. February 2012. Perturbation analysis of circadian clock degradation. Presented at the UCSD Center for Chronobiology Symposium, La Jolla, CA.

**St. John, P.C.**, M. Rodriguez-Fernandez, and F.J. Doyle III. June 2011. Advanced global optimization and sensitivity techniques for analyzing deterministic circadian models. Presented at the 12th Annual UC Systemwide Bioengineering Symposium, Santa Barbara, CA.

## Seminars

**St. John, P.C.** May 2013. Sensitivity analysis in the study of mammalian circadian rhythms. Presented at the UCSB NSF-IGERT systems biology seminar series, Santa Barbara, CA.

## Research Experience

### **University of California, Santa Barbara**

*Ph.D. Candidate*

Computational analysis of the mammalian circadian clock, with a focus on elucidating the functional design consequences of the underlying genetic regulatory network.  
Advisor: Francis J. Doyle III

Department: Chemical Engineering

**September 2010 - present**

Santa Barbara, California

<b>Tufts University</b> <i>Senior Honors Thesis</i> Catalytic Hydrodechlorination of 2-Chlorophenol using Viral-templated Palladium Nanoparticles Advisor: Hyunmin Yi Department: Chemical and Biological Engineering	<b>September 2009 - May 2010</b> Medford, Massachusetts
<b>University of California, Los Angeles</b> <i>UCLA NanoCER Program (NSF REU)</i> Encapsulation Efficiencies and Release Rates from Water-in-Oil-in-Water Nanoemulsions Advisor: Timothy Deming Department: Bioengineering	<b>June 2009 - August 2009</b> Los Angeles, California
<b>Tufts University</b> <i>Tufts Summer Scholars</i> Hydrodechlorination of 2-Chlorophenol with Palladium Nanoparticles on Genetically Modified Tobacco Mosaic Virus Scaffolds Advisor: Hyunmin Yi Department: Chemical and Biological Engineering	<b>June 2008 - August 2008</b> Medford, Massachusetts
<b>Tufts University</b> <i>Undergraduate Research Credit</i> Chemically Modified Silk Fibroin Based Scaffolds for Bone Tissue Engineering Advisor: David Kaplan Department: Biomedical Engineering	<b>October 2007 - May 2008</b> Medford, Massachusetts

## Teaching Experience

<b>University of California, Santa Barbara</b> <i>Teaching Assistant, ChE132c</i> Helped teach undergraduate statistics for two subsequent years: gave three lectures, held office hours and review sessions, and graded homeworks.	<b>January 2013 - December 2013</b> Santa Barbara, California
<b>University of California, Santa Barbara</b> <i>Teaching Assistant, ChE180a</i> Designed and ran experiments for the junior laboratory course. Also helped in grading student reports.	<b>March 2012 - June 2012</b> Santa Barbara, California

## Community Involvement

<b>Peer Review</b>	<b>January 2014-present</b>
--------------------	-----------------------------

Reviewer for Biophysical Journal; IEEE Control Systems Society Conference; 21st International Symposium on Mathematical Theory of Networks and Systems

**Scienceline "Ask A Scientist"**

**December 2010 - present**

Answers science and engineering questions posed by students and teachers from local K-12 schools.

**Website:** [www.science-line.ucsb.edu](http://www.science-line.ucsb.edu)

**UCSB Discover Engineering Weekend**

**May 2011**

Helped organize and run a weekend for local high school students to learn basic engineering principles and apply their knowledge to build miniature alternative energy cars.

## **Mentoring Experience**

Amanda Luan, Undergraduate Student, ICB SSB URAP **June 2014 - December 2014**

Lukas Widmer, Masters Student, ETH Zurich **April 2012 - February 2013**

Andrew Barisser, Rotation Student, BMSE UCSB **September 2012 - December 2012**

# Abstract

This is the second paragraph. Hello, here is some text without a meaning. This text should show what a printed text will look like at this place. If you read this text, you will get no information. Really? Is there no information? Is there a difference between this text and some nonsense like “Huardest gefburn”? Kjift – not at all! A blind text like this gives you information about the selected font, how the letters are written and an impression of the look. This text should contain all letters of the alphabet and it should be written in of the original language. There is no need for special content, but the length of words should match the language.

And after the second paragraph follows the third paragraph. Hello, here is some text without a meaning. This text should show what a printed text will look like at this place. If you read this text, you will get no information. Really? Is there no information? Is there a difference between this text and some nonsense like “Huardest gefburn”? Kjift – not at all! A blind text like this gives you information about the selected font, how the letters are written and an impression of the look. This text should contain all letters of the alphabet and it should be written in of the original language. There is no need for special content, but the length of words should match the language.

After this fourth paragraph, we start a new paragraph sequence. Hello, here is some text without a meaning. This text should show what a printed text will look like at this place. If you read this text, you will get no information. Really? Is

there no information? Is there a difference between this text and some nonsense like “Huardest gefburn”? Kjift – not at all! A blind text like this gives you information about the selected font, how the letters are written and an impression of the look. This text should contain all letters of the alphabet and it should be written in of the original language. There is no need for special content, but the length of words should match the language.

Hello, here is some text without a meaning. This text should show what a printed text will look like at this place. If you read this text, you will get no information. Really? Is there no information? Is there a difference between this text and some nonsense like “Huardest gefburn”? Kjift – not at all! A blind text like this gives you information about the selected font, how the letters are written and an impression of the look. This text should contain all letters of the alphabet and it should be written in of the original language. There is no need for special content, but the length of words should match the language.

This is the second paragraph. Hello, here is some text without a meaning. This text should show what a printed text will look like at this place. If you read this text, you will get no information. Really? Is there no information? Is there a difference between this text and some nonsense like “Huardest gefburn”? Kjift – not at all! A blind text like this gives you information about the selected font, how the letters are written and an impression of the look. This text should contain all letters of the alphabet and it should be written in of the original language. There is no need for special content, but the length of words should match the language.

# Contents

<b>1</b>	<b>Introduction</b>	<b>1</b>
1.1	Biological background . . . . .	1
1.1.1	Evolutionary history . . . . .	3
1.1.2	Mechanisms of gene regulation . . . . .	3
1.1.3	Mammalian genetic circuit . . . . .	3
1.2	Mathematical modeling . . . . .	4
1.2.1	Overview of kinetic ODE models . . . . .	4
1.2.2	Basic terms and assumptions . . . . .	5
1.2.3	Simulation methods . . . . .	6
1.2.4	ODE Sensitivity Analysis . . . . .	8
1.2.5	Previous models of circadian rhythms . . . . .	9
<b>2</b>	<b>A new model of the core circadian feedback loop</b>	<b>10</b>
2.1	Background . . . . .	10
2.1.1	Small molecule modulators . . . . .	10
2.2	Results . . . . .	13
2.2.1	A new model for period regulation . . . . .	13
2.2.2	Parameter estimation . . . . .	21
2.2.3	Model validation and dynamics . . . . .	26
2.2.4	Prediction of KL001 mechanism . . . . .	28

2.3	Conclusion	30
2.3.1	Insights into Circadian Network Design	30
2.3.2	Identifiability of model parameters	32
<b>3</b>	<b>Identifiability analysis for models of circadian rhythms</b>	<b>33</b>
3.1	Background	33
3.1.1	Identifiability analysis	34
3.2	Methods	36
3.2.1	Collocation Methods	36
3.2.2	Generating Initial Values	39
3.2.3	First Order Sensitivity Analysis	39
3.2.4	Generation of data for bootstrap methods	40
3.2.5	Calculation Times	41
3.3	Results and discussion	42
3.3.1	Effect of data quality on predictive confidence	43
3.3.2	Application to literature data for model discrimination	46
3.4	Conclusions	52
<b>4</b>	<b>Spatiotemporal separation of PER and CRY posttranslational regulation</b>	<b>55</b>
4.1	Background	55
4.1.1	Nuclear entry of PER-CRY complex	56
4.1.2	Importance of posttranslational regulators	57
4.1.3	Functional differences between PER and CRY	58
4.2	Materials and Methods	59
4.2.1	Analysis of luminescence profiles	59
4.2.2	Cost function	59
4.2.3	Parameter estimation and bootstrap analysis	63

4.2.4	Selection of parameters for FBXL3-CRY and CKI-PER mechanisms . . . . .	63
4.2.5	Numerical experiments . . . . .	64
4.3	Results and Discussion . . . . .	64
4.3.1	Opposite amplitude effects of longdaysin and KL001 . . . . .	64
4.3.2	Main period-determining perturbations . . . . .	64
4.3.3	Independent mechanisms of PER and CRY regulation . . . . .	67
4.3.4	Conclusion . . . . .	74
<b>5</b>	<b>Amplitude metrics for cellular bioluminescence reporters</b>	<b>76</b>
5.1	Motivation, link to previous chapter . . . . .	76
5.1.1	Different enzymes control circadian rhythms at different phases	76
5.1.2	Perturbations likely have a time-dependent effect on amplitude .	77
5.1.3	Comparison of Ukai vs Pulivarthy 2007 . . . . .	77
5.2	Single cell amplitude metrics . . . . .	78
5.2.1	Definition of amplitude metric . . . . .	78
5.2.2	Finite difference ARC . . . . .	78
5.2.3	Derivation of sensitivity-based method . . . . .	79
5.3	Population-level models . . . . .	79
5.3.1	Definitions and diffusion-convection equation . . . . .	80
5.3.2	Circular statistics . . . . .	80
5.3.3	Inverting $p(\theta, \hat{t})$ . . . . .	80
5.3.4	Calculating $\bar{x}(\hat{t})$ and $\hat{x}(\hat{t})$ . . . . .	81
<b>6</b>	<b>Decay rate as proxy for cellular noise</b>	<b>82</b>
<b>7</b>	<b>Conclusions and future work</b>	<b>83</b>
7.1	Continuation of collaboration with Andrew . . . . .	83
7.1.1	Experimental validation of model predictions . . . . .	83

7.1.2	Prediction of fasting perturbations . . . . .	84
7.1.3	Validity of step vs pulse perturbation . . . . .	85
7.2	Amplitude maximization through therapeutic treatment . . . . .	85
7.2.1	Optimal control strategies to maximize peripheral clock amplitude . . . . .	86
7.2.2	Fewest treatments, combinatorial perturbations, etc. . . . .	86
7.3	Iterative optimization of network topology . . . . .	87
7.3.1	(Idea from Mitsubishi proposal) . . . . .	87
7.3.2	Design machine-learning algorithm to find optimum model structure . . . . .	87

# List of Figures

1.1	A biological feed forward controller	2
2.1	Model Connectivity	14
2.2	Degradation Profiles	15
2.3	Time Course Plots	27
2.4	Model Validation	28
2.5	Model Prediction of the KL001 Mechanism	29
2.6	Simultaneous Knockdown of <i>Cry1</i> and <i>Cry2</i>	31
2.7	First Order Relative Period Sensitivities	31
3.1	Parameter estimation and bootstrap methods flowchart	44
3.2	Time-course Profiles of the State Trajectories for Per mRNA	45
3.3	Parameter and Sensitivity Identifiability for Increasing Error	47
3.4	Effect of High-resolution Sampling on Identifiability	48
3.5	Identifiability Comparison of Two Model Structures	49
3.6	Time-Series Dynamics of Fitted Models	53
4.1	Small molecule targets	57
4.2	Analysis of circadian reporter luminescence data	60
4.3	Different amplitude effect of small molecule circadian modulators targeting CKI-PER and FBXL3-CRY	65
4.4	Fitted trajectories from bootstrap runs	66

4.5	Bootstrap confidence intervals in relative period sensitivities . . . . .	68
4.6	Bootstrap predictions of circadian actions of FBXL3-CRY and CKI-PER pathways . . . . .	69
4.7	Predictions of KL001 and longdaysin results . . . . .	71
4.8	Comparison of the effects of KL001 and longdaysin . . . . .	71
4.9	Effect of cytoplasmic PER stabilization on period and E box transcription amplitude . . . . .	72
4.10	Comparison of two candidate mechanisms for CKI inhibition . . . . .	73

# Chapter 1

## Introduction

### 1.1 Biological background

Systems biology is a multidisciplinary field, drawing from biology, mathematics, and computer science. In this section, I first provide a background on the biology of circadian rhythms, followed by previous literature on computational modeling.

Ecological competition drives species to optimize their survival and reproduction in a particular environmental niche. Aspects of their environment, including temperature, resource availability, and sunlight are all important factors in determining an individual's success.

In nearly all environments, however, these factors vary greatly from hour to hour and month to month. While food or sunlight might be plentiful during daylight hours, the threat of predators might peak as well. Fortunately, while these critical parameters undergo sharp changes, they do so with a predictable and repeatable schedule. It is not surprising that, in optimizing their survival in an oscillating environment, species have developed a means to predict changes and to ready themselves for the correct behavior.

Biological rhythms are classified as *circadian* if they display a number of defining

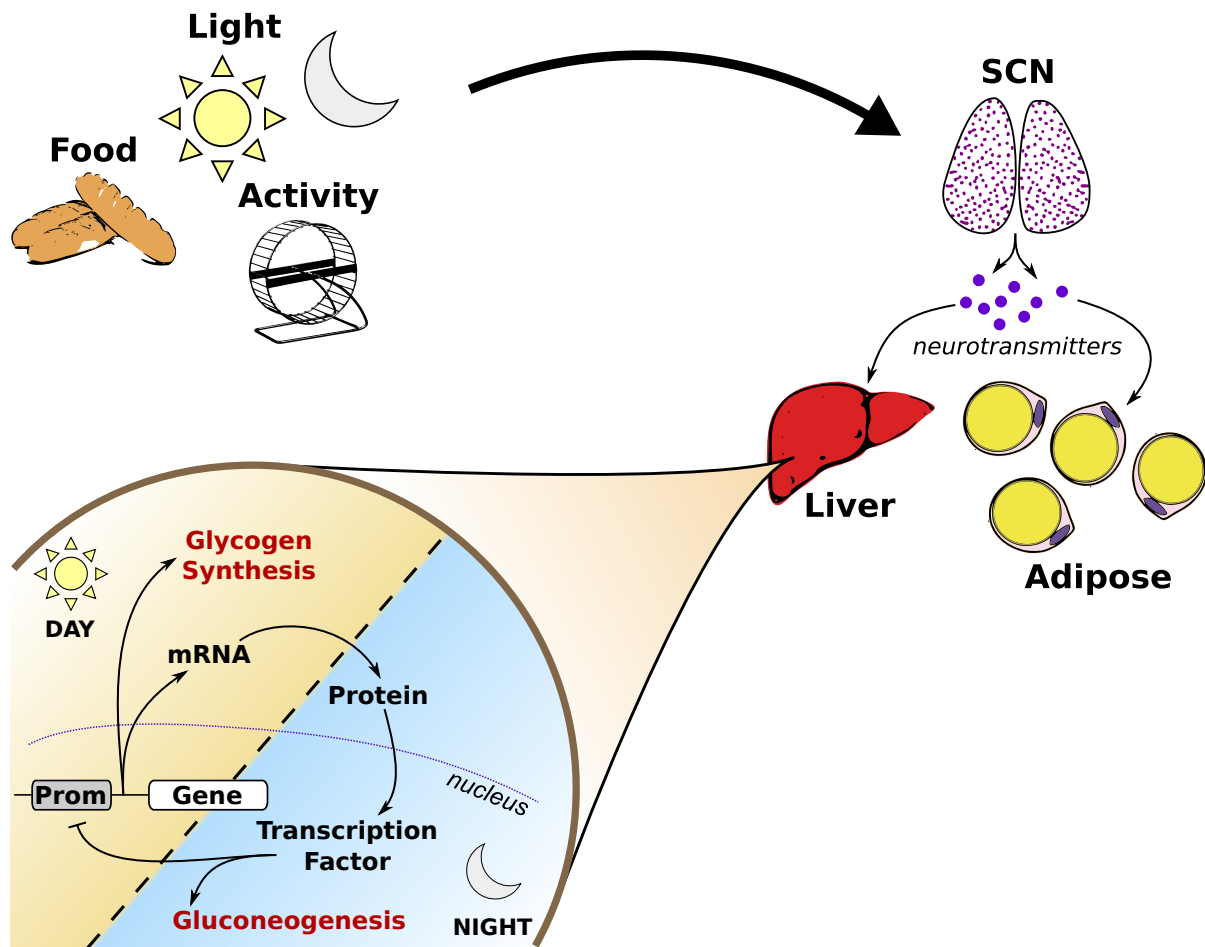


Figure 1.1: A biological feed forward controller. Circadian rhythms

characteristics:

- They are *endogenous*, meaning they continue to oscillate even when the organism is isolated from its environment
- They are temperature compensated, maintaining a consistent period for moderate changes in average temperature
- They are *entrainable*, meaning they can adjust their phase and period in response to a changing in environmental signal
- They oscillate with a roughly 24 hour period [1].

### **1.1.1 Evolutionary history**

Hello, here is some text without a meaning. This text should show what a printed text will look like at this place. If you read this text, you will get no information. Really? Is there no information? Is there a difference between this text and some nonsense like “Huardest gefburn”? Kjift – not at all! A blind text like this gives you information about the selected font, how the letters are written and an impression of the look. This text should contain all letters of the alphabet and it should be written in of the original language. There is no need for special content, but the length of words should match the language.

### **1.1.2 Mechanisms of gene regulation**

Hello, here is some text without a meaning. This text should show what a printed text will look like at this place. If you read this text, you will get no information. Really? Is there no information? Is there a difference between this text and some nonsense like “Huardest gefburn”? Kjift – not at all! A blind text like this gives you information about the selected font, how the letters are written and an impression of the look. This text should contain all letters of the alphabet and it should be written in of the original language. There is no need for special content, but the length of words should match the language.

### **1.1.3 Mammalian genetic circuit**

Hello, here is some text without a meaning. This text should show what a printed text will look like at this place. If you read this text, you will get no information. Really? Is there no information? Is there a difference between this text and some nonsense like “Huardest gefburn”? Kjift – not at all! A blind text like this gives you information about the selected font, how the letters are written and an impression of

the look. This text should contain all letters of the alphabet and it should be written in of the original language. There is no need for special content, but the length of words should match the language.

## 1.2 Mathematical modeling

Hello, here is some text without a meaning. This text should show what a printed text will look like at this place. If you read this text, you will get no information. Really? Is there no information? Is there a difference between this text and some nonsense like “Huardest gefburn”? Kjift – not at all! A blind text like this gives you information about the selected font, how the letters are written and an impression of the look. This text should contain all letters of the alphabet and it should be written in of the original language. There is no need for special content, but the length of words should match the language.

### 1.2.1 Overview of kinetic ODE models

Hello, here is some text without a meaning. This text should show what a printed text will look like at this place. If you read this text, you will get no information. Really? Is there no information? Is there a difference between this text and some nonsense like “Huardest gefburn”? Kjift – not at all! A blind text like this gives you information about the selected font, how the letters are written and an impression of the look. This text should contain all letters of the alphabet and it should be written in of the original language. There is no need for special content, but the length of words should match the language.

### **Spectrum of modeling methods (detail vs. scope)**

Hello, here is some text without a meaning. This text should show what a printed text will look like at this place. If you read this text, you will get no information. Really? Is there no information? Is there a difference between this text and some nonsense like “Huardest gefburn”? Kjift – not at all! A blind text like this gives you information about the selected font, how the letters are written and an impression of the look. This text should contain all letters of the alphabet and it should be written in of the original language. There is no need for special content, but the length of words should match the language.

#### **1.2.2 Basic terms and assumptions**

Hello, here is some text without a meaning. This text should show what a printed text will look like at this place. If you read this text, you will get no information. Really? Is there no information? Is there a difference between this text and some nonsense like “Huardest gefburn”? Kjift – not at all! A blind text like this gives you information about the selected font, how the letters are written and an impression of the look. This text should contain all letters of the alphabet and it should be written in of the original language. There is no need for special content, but the length of words should match the language.

#### **Mass action**

Hello, here is some text without a meaning. This text should show what a printed text will look like at this place. If you read this text, you will get no information. Really? Is there no information? Is there a difference between this text and some nonsense like “Huardest gefburn”? Kjift – not at all! A blind text like this gives you information about the selected font, how the letters are written and an impression of

the look. This text should contain all letters of the alphabet and it should be written in of the original language. There is no need for special content, but the length of words should match the language.

### **Michealis-Menten**

Hello, here is some text without a meaning. This text should show what a printed text will look like at this place. If you read this text, you will get no information. Really? Is there no information? Is there a difference between this text and some nonsense like “Huardest gefburn”? Kjift – not at all! A blind text like this gives you information about the selected font, how the letters are written and an impression of the look. This text should contain all letters of the alphabet and it should be written in of the original language. There is no need for special content, but the length of words should match the language.

### **Hill-type**

Hello, here is some text without a meaning. This text should show what a printed text will look like at this place. If you read this text, you will get no information. Really? Is there no information? Is there a difference between this text and some nonsense like “Huardest gefburn”? Kjift – not at all! A blind text like this gives you information about the selected font, how the letters are written and an impression of the look. This text should contain all letters of the alphabet and it should be written in of the original language. There is no need for special content, but the length of words should match the language.

#### **1.2.3 Simulation methods**

Hello, here is some text without a meaning. This text should show what a printed text will look like at this place. If you read this text, you will get no information.

Really? Is there no information? Is there a difference between this text and some nonsense like “Huardest gefburn”? Kjift – not at all! A blind text like this gives you information about the selected font, how the letters are written and an impression of the look. This text should contain all letters of the alphabet and it should be written in of the original language. There is no need for special content, but the length of words should match the language.

### **Numerical solution of nonlinear ODEs**

Hello, here is some text without a meaning. This text should show what a printed text will look like at this place. If you read this text, you will get no information. Really? Is there no information? Is there a difference between this text and some nonsense like “Huardest gefburn”? Kjift – not at all! A blind text like this gives you information about the selected font, how the letters are written and an impression of the look. This text should contain all letters of the alphabet and it should be written in of the original language. There is no need for special content, but the length of words should match the language.

### **Boundary value problem for limit cycle models**

Hello, here is some text without a meaning. This text should show what a printed text will look like at this place. If you read this text, you will get no information. Really? Is there no information? Is there a difference between this text and some nonsense like “Huardest gefburn”? Kjift – not at all! A blind text like this gives you information about the selected font, how the letters are written and an impression of the look. This text should contain all letters of the alphabet and it should be written in of the original language. There is no need for special content, but the length of words should match the language.

### **1.2.4 ODE Sensitivity Analysis**

Hello, here is some text without a meaning. This text should show what a printed text will look like at this place. If you read this text, you will get no information. Really? Is there no information? Is there a difference between this text and some nonsense like “Huardest gefburn”? Kjift – not at all! A blind text like this gives you information about the selected font, how the letters are written and an impression of the look. This text should contain all letters of the alphabet and it should be written in of the original language. There is no need for special content, but the length of words should match the language.

#### **ODEs in general**

Hello, here is some text without a meaning. This text should show what a printed text will look like at this place. If you read this text, you will get no information. Really? Is there no information? Is there a difference between this text and some nonsense like “Huardest gefburn”? Kjift – not at all! A blind text like this gives you information about the selected font, how the letters are written and an impression of the look. This text should contain all letters of the alphabet and it should be written in of the original language. There is no need for special content, but the length of words should match the language.

#### **Period sensitivity**

Hello, here is some text without a meaning. This text should show what a printed text will look like at this place. If you read this text, you will get no information. Really? Is there no information? Is there a difference between this text and some nonsense like “Huardest gefburn”? Kjift – not at all! A blind text like this gives you information about the selected font, how the letters are written and an impression of the look. This text should contain all letters of the alphabet and it should be written

in of the original language. There is no need for special content, but the length of words should match the language.

## **PRCs**

Hello, here is some text without a meaning. This text should show what a printed text will look like at this place. If you read this text, you will get no information. Really? Is there no information? Is there a difference between this text and some nonsense like “Huardest gefburn”? Kjift – not at all! A blind text like this gives you information about the selected font, how the letters are written and an impression of the look. This text should contain all letters of the alphabet and it should be written in of the original language. There is no need for special content, but the length of words should match the language.

### **1.2.5 Previous models of circadian rhythms**

Hello, here is some text without a meaning. This text should show what a printed text will look like at this place. If you read this text, you will get no information. Really? Is there no information? Is there a difference between this text and some nonsense like “Huardest gefburn”? Kjift – not at all! A blind text like this gives you information about the selected font, how the letters are written and an impression of the look. This text should contain all letters of the alphabet and it should be written in of the original language. There is no need for special content, but the length of words should match the language.

# Chapter 2

## A new model of the core circadian feedback loop<sup>1</sup>

### 2.1 Background

#### 2.1.1 Small molecule modulators

Circadian rhythms help to regulate metabolic homeostasis, and therefore compromised circadian oscillations often result in negative health consequences. Since circadian rhythms may be damped by lifestyle factors, many researchers have begun searching for pharmacological agents which might alter circadian rhythmicity. Several proof-of-concept molecules have been found which cause dose-dependent period change in cultured fibroblasts [2]. While chemical biology approaches are able to localize the effects of these molecules to specific targets in the circadian network, it is often difficult to reconcile individual rate changes with the observed systems-level changes in period or amplitude. Mathematical models are therefore essential

---

<sup>1</sup>Portions of this chapter are published in T. Hirota, J. W. Lee, P. C. St. John, M. Sawa, K. Iwaisako, T. Noguchi, P. Y. Pongsawakul, T. Sonntag, D. K. Welsh, D. A. Brenner, F. J. Doyle, P. G. Schultz, and S. A. Kay, "Identification of Small Molecule Activators of Cryptochrome," *Science*, vol. 337, pp. 1094–1097, July 2012.

to understanding the effects of such drugs, as they are able to verify that hypothesized mechanisms of action are mathematically consistent. Furthermore, mathematical models provide a systematic framework by which to examine consequences of various mechanistic assumptions - many of which can be subsequently verified by experimental inquiry. The search for small molecule modulators of circadian rhythms therefore yields the added benefit of strengthening our knowledge of the core clock feedback circuit, as inconsistencies between assumed kinetics and experimental results often lead to a more refined knowledge of the network's dynamics.

In this chapter, I describe a collaborative project in which experimental results inspired the creation of a new model of the core mammalian feedback network. A new small molecule modulator of cryptochrome, KL001, was identified through forward chemical genetic screening [3]. The compound was found to simultaneously increase the half-life of CRY and cause period lengthening. In order to explain these new experimental results while maintaining consistency with published evidence, I constructed a simple mathematical model of the Per/Cry negative feedback loop.

The functional roles of the cryptochrome isoforms (*Cry1* and *Cry2*) in circadian rhythms have long eluded biologists, as although they share a similar structure, perturbations to these genes typically result in opposite trends [4]. Existing genetic evidence and siRNA knockdown studies agree that while suppressing *Cry1* leads to shorter periods, suppressing *Cry2* leads to longer periods [5, 6]. However, some evidence shows the similarity between the two *Crys*. The knockouts  $Cry1^{+/-} \ll Cry2^{-/-}$  and  $Cry1^{-/-} Cry2^{+/-}$  both show shorter wheel-running activity than their respective WT/double knockouts  $Cry1^{+/+} Cry2^{-/-}$  and  $Cry1^{-/-} Cry2^{+/+}$  [5]. Using new data from the application of KL001 together with existing experimental results, I developed a hypothesized mechanism to reconcile these seemingly contradictory results:

## Network structure

In the core feedback loop, Per and Cry transcription is activated by the CLOCK-BMAL1 complex. The protein products of these genes are transported to the nucleus after a time delay and bind to CLOCK-BMAL1, repressing their own transcription. Evidence indicates that an interaction of PER and CRY proteins is required for the timely nuclear entry of both proteins [7, 8, 9]. I therefore assume that PER and CRY bind and enter the nucleus in a 1:1 stoichiometric ratio, similar to more complicated models of mammalian circadian rhythms [10, 11, 12].

## Protein stoichiometry

Quantitative protein assays have revealed that the PER proteins are present at levels nearly ten times less than the CRYs, and are completely consumed at their trough. The CRYs, on the other hand, only fall to about one quarter of their peak value [13]. These results indicate that PER is the rate-limiting component for nuclear entry. This configuration explains why, since /it Cry is in excess, a knockout of either *Cry* does not lead to loss of function at the tissue level. Additionally *Cry1*, the more dominant repressor, is consistently found at higher levels than *Cry2*. However, since the ratio of nuclear to total protein is nearly equivalent for CRY1 and CRY2, PER must import each with equal affinity [13, 14].

## Importance of degradation

Studies of the simplest cellular oscillators have illustrated the importance of the degradation of repressor complexes in determining the period of oscillation [15]. In the mammalian circadian clock, FBXL3 has been indicated as a key protein in clearing the nucleus of CRY, and siRNA knockdowns of *Fbxl3* result in period lengthening [6]. While FBXL3 localizes primarily in the nucleus, CRY2 possesses a distinct phosphorylation domain that flags it for cytosolic proteolysis [16]. Knocking down this

domain shortens the period, indicating that degradation rates play a major role in determining the oscillatory period and that stabilization in the cytosol and nucleus are likely not equivalent.

### Key time delays

Similar to *Drosophila*, mammalian circadian oscillations are generated by three main time delays in the negative feedback loop: mRNA transcription, nuclear localization of protein, and degradation of the nuclear complexes [17]. In order to capture these dynamics without introducing unnecessary stiffness, I explicitly consider only the concentrations of nuclear mRNA, cytosolic unbound protein, and nuclear protein complexes.

## 2.2 Results

### 2.2.1 A new model for period regulation

Since the circadian clock is largely insensitive to the total amount *Cry*, it follows that the core negative loop is comprised of two redundant coupled inhibitory mechanisms. The natural periods of these two loops (running in isolation of the other) can be inferred from their corresponding knockout phenotype, i.e., the CRY1 feedback loop has a long period, while the CRY2 loop has a short period. In the wild-type phenotype, the two isoforms of CRY must compete for the available PER, and thus the nuclear CRY1/CRY2 levels are constrained with a ratio proportional to their relative expression. This suggests that the period of the clock is governed by the nuclear CRY1/CRY2 ratio, where higher amounts of *Cry1* shift the clock closer to the *Cry2*<sup>-/-</sup> phenotype, and higher amounts of *Cry2* shift the clock closer to the *Cry1*<sup>-/-</sup> phenotype, described in figure 2.1.

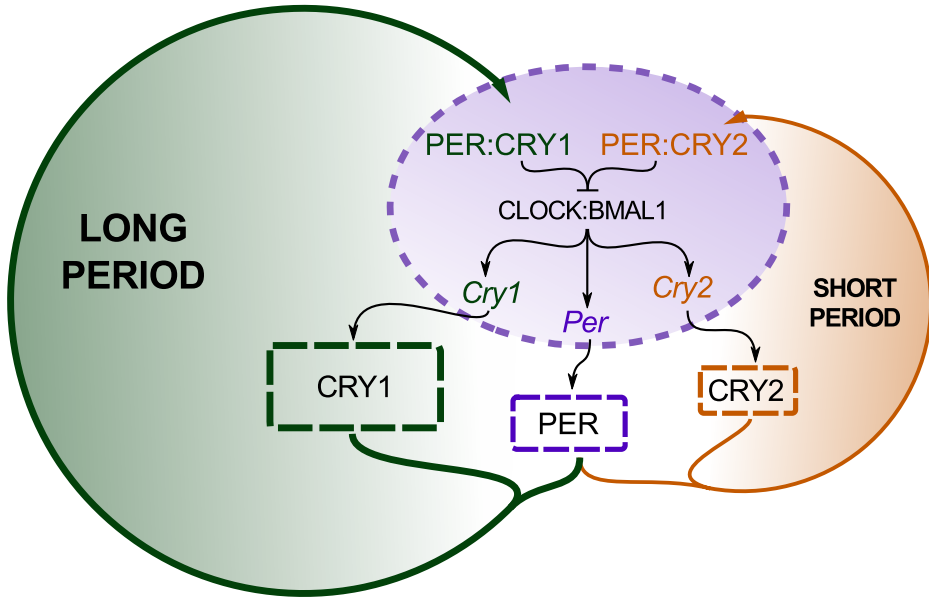


**Figure 2.1: Model Connectivity.** Schematic for the core negative feedback loop, consisting of the two redundant *Cry* mechanisms. The wild-type period, consisting of both loops, is a balance between the short and long oscillations.

### The CRY1/CRY2 ratio

*In silico* modeling was used to test the feasibility of the above hypothesis, and to investigate possible mechanisms by which the CRY1/CRY2 ratio might control the period of oscillations. The model uses eight state variables for the three mRNA species (*Per*, *Cry1*, and *Cry2*), three cytosolic proteins, and two nuclear proteins. The differential equations for each state were formulated using standard Hill-type repression, Michaelis-Menten, and mass action kinetics. The 21 unknown kinetic parameters were found by fitting the stoichiometric data from [13], requiring correct periods for the *Cry1*<sup>-/-</sup> and *Cry2*<sup>-/-</sup> knockouts.

I investigated two possible mechanisms to explain the long/short period phenotype of the CRY1/CRY2 loops. First, following experimental evidence, I allowed CRY1 and CRY2 to have different inhibitory efficiency [18]. However, optimizations with this structure were unable to find a parameter set with appropriate period sen-

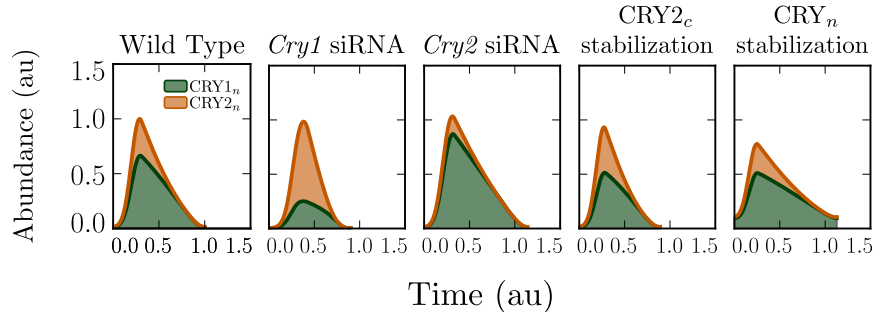


**Figure 2.2: Degradation Profiles.** Time course plots of the simulated total nuclear repressor concentration for the degradation model under various clock conditions. The relative contribution of CRY1 and CRY2 are shaded green and orange, respectively. Longer periods occur when a higher percentage of the nuclear complex is CRY1, taking longer to degrade.

sivities, described in section 2.2.2. Instead, I investigated whether the difference in potency between *Crys* could be explained through difference in degradation rates. To this end, I allowed the degradation rates of nuclear CRY1 and CRY2 to differ, while holding their inhibition constants equal. Using this configuration, the structure was able to fit the experimental sensitivities. In the optimized parameter set, the degradation rate of nuclear CRY2 is higher than that of CRY1, such that for a constant total nuclear CRY, higher fractions of CRY2 cause the repressive complexes to be cleared faster. Since PER is the limiting reagent in nuclear entry, the amount of total CRY that enters the nucleus is largely insensitive to perturbations in cytosolic CRY expression. In effect, the two isoforms of CRY must compete for the available PER, and thus the nuclear CRY1/CRY2 levels are constrained with a ratio proportional to their relative expression. The period of the clock is thus governed by the nuclear CRY1/CRY2 ratio, where higher amounts of *Cry1* shift the clock closer to the *Cry2*<sup>-/-</sup> phenotype, and higher amounts of *Cry2* shift the clock closer to the *Cry1*<sup>-/-</sup> phenotype. Figure 2.2 shows the time varying total complex concentration under various perturbations, with the relative contributions from CRY1 and CRY2 highlighted.

## Model equations

The model is formulated as set of 8 ordinary differential equations shown in tables 2.1 and 2.2. Additional assumptions made while formulating the model equations are listed below:

- For simplicity and ease of parameter estimation, the model only considers the three genes *Per*, *Cry1*, and *Cry2*, not explicitly considering the three known isoforms of *Per*.
- EBOX activators *Clock* and *Bmal1* are considered constitutively expressed and are represented by the  $v_{txn}$  parameters.
- Repression of CLOCK-BMAL1 activity is attained through Hill-type inhibition. The Hill coefficient is fixed at 3, which was found to provide sufficient non-linearity for oscillations. See below for the derivation of the repressor input function used in tables S2A and S2B.
- The degradation of the mRNA species and cytoplasmic proteins is assumed to follow standard Michaelis-Menten kinetics.
- The degradation kinetics of the nuclear proteins are assumed to follow Michaelis-Menten kinetics. Because both  $CRY1_n$  and  $CRY2_n$  are thought to be degraded by the same pathway in the nucleus, kinetic equations using the *pseudo* steady-state hypothesis were derived for two substrates sharing the same enzyme. As a result, each *Cry* isoform acts as an inhibitor to the other's degradation.

**Table 2.1: Model Equations for the Degradation Model.** Lower case letters ( $p$ : *Per*,  $c1$ : *Cry1*,  $c2$ : *Cry2*) are mRNA state variables. Uppercase letters ( $P$ : *PER*,  $C1$ : *CRY1*,  $C2$ : *CRY2*) are the free (cytosolic) proteins.  $C1N$ : *CRY1* and  $C2N$ : *CRY2* are the nuclear proteins.

$$\frac{dp}{dt} = \frac{v_{txn,p}}{k_{txn,p} + (C1N + C2N)^3} - \frac{v_{deg,p} p}{k_{deg,p} + p} \quad (2.1)$$

$$\frac{dc1}{dt} = \frac{v_{txn,c1}}{k_{txn,c} + (C1N + C2N)^3} - \frac{v_{deg,c1} c1}{k_{deg,c} + c1} \quad (2.2)$$

$$\frac{dc2}{dt} = \frac{v_{txn,c2}}{k_{txn,c} + (C1N + C2N)^3} - \frac{v_{deg,c2} c2}{k_{deg,c} + c2} \quad (2.3)$$

$$\begin{aligned} \frac{dP}{dt} = k_{tln,p} p - \frac{v_{deg,p} P}{k_{deg,p} + P} - v_{a,CP} P C1 + v_{d,CP} C1N \\ - v_{a,CP} P C2 + v_{d,CP} C2N \end{aligned} \quad (2.4)$$

$$\frac{dC1}{dt} = c1 - \frac{v_{deg,c1} C1}{k_{deg,c} + C1} - v_{a,CP} P C1 + v_{d,CP} C1N \quad (2.5)$$

$$\frac{dC2}{dt} = c2 - \frac{v_{deg,c2} C2}{k_{deg,c} + C2} - v_{a,CP} P C2 + v_{d,CP} C2N \quad (2.6)$$

$$\frac{dC1N}{dt} = - \frac{v_{deg,CP} C1N}{k_{deg,CP} + C1N + C2N} + v_{a,CP} P C1 - v_{d,CP} C1N \quad (2.7)$$

$$\frac{dC2N}{dt} = - \frac{(v_{deg,CP} m_{C2N}) C2N}{k_{deg,CP} + C2N + C1N} + v_{a,CP} P C2 - v_{d,CP} C2N \quad (2.8)$$

**Table 2.2: Changed Equations for the Activation-based Model.** The remainder of the model equations (not duplicated below) are found in table 2.1

$$\frac{dp}{dt} = \frac{v_{txn,p}}{k_{txn,p} + (m_{C2N} C1N + C2N)^3} - \frac{v_{deg,p} p}{k_{deg,p} + p} \quad (2.1^*)$$

$$\frac{dc1}{dt} = \frac{v_{txn,c1}}{k_{txn,c} + (m_{C2N} C1N + C2N)^3} - \frac{v_{deg,c1} c1}{k_{deg,c} + c1} \quad (2.2^*)$$

$$\frac{dc2}{dt} = \frac{v_{txn,c2}}{k_{txn,c} + (m_{C2N} C1N + C2N)^3} - \frac{v_{deg,c2} c2}{k_{deg,c} + c2} \quad (2.3^*)$$

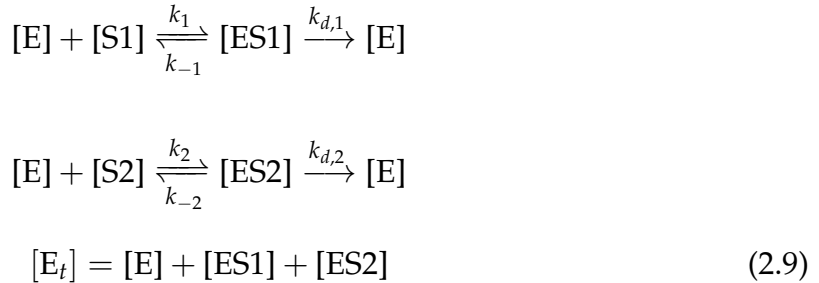
$$\frac{dC2N}{dt} = - \frac{v_{deg,CP} C2N}{k_{deg,CP} + C2N + C1N} + v_{a,CP} P C2 - v_{d,CP} C2N \quad (2.8^*)$$

**Table 2.3: Parameter Set.** Parameters for model described in table 2.1.

	Parameter	Description	Degradation	Activation
1	$v_{\text{txn,p}}$	<i>Per</i> Transcription rate	0.195	0.276
2	$v_{\text{txn,c1}}$	<i>Cry1</i> Transcription rate	0.131	0.062
3	$v_{\text{txn,c2}}$	<i>Cry1</i> Transcription rate	0.114	0.053
4	$k_{\text{txn,p}}$	<i>Per</i> Repression constant	0.425	0.425
5	$k_{\text{txn,c}}$	<i>Cry1/2</i> Repression constant	0.259	0.262
6	$v_{\text{deg,p}}$	<i>Per</i> Max degradation rate	0.326	0.472
7	$v_{\text{deg,c1}}$	<i>Cry1</i> Max degradation rate	0.676	0.322
8	$v_{\text{deg,c2}}$	<i>Cry2</i> Max degradation rate	0.608	0.290
9	$k_{\text{deg,p}}$	<i>Per</i> Degradation constant	0.011	0.024
10	$k_{\text{deg,c}}$	<i>Cry1/2</i> Degradation constant	1.149	0.809
11	$v_{\text{deg,P}}$	Max PERc degradation rate	2.970	2.970
12	$k_{\text{deg,P}}$	PERc degradation constant	0.034	0.034
13	$v_{\text{deg,C1}}$	Max CRY1c degradation rate	1.523	1.048
14	$v_{\text{deg,C2}}$	Max CRY2c degradation rate	1.686	1.134
15	$k_{\text{deg,C}}$	CRYc degradation constant	2.017	2.028
16	$v_{\text{deg,CP}}$	CRYn degradation rate	0.101	0.070
17	$m_{\text{C2N}}$	CRY2n degradation multiplier	3.318	3.334
18	$k_{\text{deg,CP}}$	CRYn degradation constant	0.053	0.053
19	$v_{\text{a,CP}}$	CRYn association rate	0.041	0.028
20	$v_{\text{d,CP}}$	CRYn dissociation rate	0.002	0.001
21	$k_{\text{tln,p}}$	PER translation rate	3.000	1.000

### Derivation of a shared enzyme degradation rate

To find the rate equations associated with a shared-enzyme degradation mechanism, we derive them from the equilibrium relationships:



The end goal is the degradation rates of the two enzyme complexes:

$$\begin{aligned}
 r_{d,1} &= k_{d,1} [ES1] \\
 r_{d,2} &= k_{d,2} [ES2]
 \end{aligned} \tag{2.10}$$

We invoke the standard pseudo steady-state assumption and set  $\frac{d[ES]}{dt} = 0$ , and obtain the following production = consumption equalities for [ES1]:

$$k_1[E][S] = k_{-1}[ES1] + k_{d,1}[ES1] \tag{2.11}$$

Solving equation (2.11) for ES1 and substituting in equation (2.9), we obtain

$$\left( \frac{k_{-1} + k_{d,1}}{k_1} \right) [ES1] = ([E_t] - [ES1] - [ES2]) [S1]$$

After defining a useful combined rate constant,

$$K_1 \equiv \frac{k_{-1} + k_{d,1}}{k_1}$$

we can further simplify

$$\begin{aligned} K_1[ES1] + [S1][ES1] &= ([E_t] - [ES2])[S1] \\ [ES1] &= \frac{([E_t] - [ES2])[S1]}{K_1 + [S1]} \end{aligned} \quad (2.12)$$

If we perform the same operations for [ES2] and plug them into equation (2.12).

$$\begin{aligned} [ES1] &= \frac{\left(E_t - \frac{([E_t] - [ES1])[S2]}{K_2 + [S2]}\right) S1}{K_1 + [S1]} \\ [ES1] &= \frac{[E]_t[S1]}{K_1 + [S1]} - \frac{[E]_t[S1][S2]}{(K_1 + [S1])(K_2 + [S2])} + \frac{[ES1][S1][S2]}{(K_1 + [S1])(K_2 + [S2])} \\ [ES1] &= \left(\frac{[E]_t[S1]}{K_1 + [S1]}\right) \left(\frac{1 - \frac{[S2]}{K_2 + [S2]}}{1 - \frac{[S1][S2]}{(K_1 + [S1])(K_2 + [S2])}}\right) \end{aligned} \quad (2.13)$$

If we pull the second fraction from (equation (2.13)) into the denominator of the first, we can simplify further.

$$\begin{aligned} [ES1] &= \frac{[E]_t[S1]}{\left(\frac{K_1 + [S1] - \frac{[S1][S2]}{K_2 + [S2]}}{1 - \frac{[S2]}{K_2 + [S2]}}\right)} \\ [ES1] &= \frac{[E]_t[S1]}{\left(\frac{K_2 + [S2]}{K_2}\right) \left(K_1 + [S1] - \frac{[S1][S2]}{K_2 + [S2]}\right)} \\ [ES1] &= \frac{K_2[E]_t[S1]}{(K_1 + [S1])(K_2 + [S2]) - [S1][S2]} \\ [ES1] &= \frac{K_2[E]_t[S1]}{K_1 K_2 + K_2[S1] + K_1[S2]} \\ [ES1] &= \frac{K_2[E]_t[S1]}{K_1 K_2 + K_2[S1] + K_1[S2]} \end{aligned}$$

Dividing top and bottom by K2:

$$[ES1] = \frac{[E]_t[S1]}{K_1 + [S1] + \frac{K_1}{K_2}[S2]} \quad (2.14)$$

Substituting (equation (2.14)) into (equation (2.10)) and setting  $K_1 = K_2$ ,  $k_{d,1} \neq k_{d,2}$ , we obtain the final shared rate laws (with an equivalent analysis for [ES2])

$$r_{d,1} = \frac{V_{\max,1}[\text{S1}]}{K_M + [\text{S1}] + [\text{S2}]}$$

$$r_{d,2} = \frac{V_{\max,2}[\text{S2}]}{K_M + [\text{S1}] + [\text{S2}]}$$

### Derivation of Hill-type repression formulas

To derive the equations for the Hill-type inhibition, allowing for different repressive activities (table 2.2), we start with the standard equation for Hill-type regulation:

$$\frac{v_{\max}[A]^n}{K_m^n + [A]^n} \quad (2.15)$$

Allowing for competitive inhibition with two inhibitors,  $K_m$  is replaced with the apparent Michaelis-Menten constant

$$K_m^{\text{app}} = K_m \left( 1 + \frac{[I_1]}{K_{i,1}} + \frac{[I_2]}{K_{i,2}} \right) \quad (2.16)$$

By assuming constitutive activator concentrations and non-dimensionalizing  $[I^*] = \frac{[I]}{K_{i,2}}$ ,  $m = \frac{K_{i,2}}{K_{i,1}}$ :

$$\frac{v_{\max^*}}{K_m^* + (m [I_1^*] + [I_2^*])^n}$$

Assuming equal repressive activity ( $K_{i,2} = K_{i,1}$ ),  $m = 1$ , we obtain the rate equation used in the degradation model.

### 2.2.2 Parameter estimation

The model equations, specifying the state and parameter dependent time derivatives of each concentration variable, were written in python using the CasADi computer

algebra package [19]. The model was simulated using the SUNDIALS suite of ODE solvers [20]. A parameter-dependent cost function was developed that assigns numerical values reflecting how well a parameter set fits desired features, taken from [13]. The first step in the cost function evaluation is the numerical solution of the limit cycle, described previously [21]. If a limit cycle was unable to be found, the cost function returns a maximum value. Otherwise, the cost function returns a squared difference from the desired value. A priority weight was also attached to each cost entry, such that more important costs would be prioritized. A description of each entry in the cost function, along with the value for experimental and final model is shown in table 2.4 (degradation-based model, table 2.1; activation-based model, table 2.2). To minimize the cost function, we employed a genetic algorithm method used previously for optimizing circadian parameters [11]. In the method, 5000 solutions are calculated at random parameter values within feasible bounds. Those with the best cost function scores are kept and used to generate subsequent solutions. This procedure is iterated for up to 2000 generations, or until convergence criteria are met.

**Table 2.4: Summary of Cost Function Entries.** The weights for each entry were chosen based on the relative importance of the desired behavior. Entries 1-9 and 12-16 were obtained from the data presented in [13]. SiRNA sensitivities were obtained were taken from [6].

---

	Description	Weight	Desired	Degradation	Activation
1	per mRNA peak-trough ratio	0.5	> 20	large	large
$\frac{y_{\max}(Per)}{y_{\min}(Per)}$					

---

Description		Weight	Desired	Degradation	Activation
2	<i>Cry1</i> mRNA peak-trough ratio	0.5	2.155	8.942	3.748
	$\frac{y_{\max}(Cry1)}{y_{\min}(Cry1)}$				
3	<i>Cry2</i> mRNA peak-trough ratio	0.5	2.236	7.813	3.484
	$\frac{y_{\max}(Cry2)}{y_{\min}(Cry2)}$				
4	PER protein peak to trough ratio	5	> 20	large	large
	$\frac{y_{\max}(\text{PER})}{y_{\min}(\text{PER})}$				
5	CRY1 protein peak-trough ratio	3	3.247	6.385	1.847
	$\frac{y_{\max}(\text{CRY1})}{y_{\min}(\text{CRY1})}$				
6	CRY2 protein peak-trough ratio	3	1.975	8.094	2.347
	$\frac{y_{\max}(\text{CRY2})}{y_{\min}(\text{CRY2})}$				

---

Description		Weight	Desired	Degradation	Activation
7	Fraction PER of total protein	3	0.105	0.169	0.073
	$\frac{y_{\max}(\text{PER})}{y_{\max}(\text{PER}) + y_{\max}(\text{CRY1}) + y_{\max}(\text{CRY2})}$				
8	Fraction CRY1 of total protein	3	0.555	0.473	0.554
	$\frac{y_{\max}(\text{CRY1})}{y_{\max}(\text{PER}) + y_{\max}(\text{CRY1}) + y_{\max}(\text{CRY2})}$				
9	Fraction CRY2 of total protein	3	0.341	0.358	0.373
	$\frac{y_{\max}(\text{CRY2})}{y_{\max}(\text{PER}) + y_{\max}(\text{CRY1}) + y_{\max}(\text{CRY2})}$				
10	<i>Cry1</i> siRNA period sensitivity	5	< 0	< 0	> 0
	$\frac{\partial T}{\partial v_{\text{deg},\text{c1}}}$				
11	<i>Cry2</i> siRNA period sensitivity	5	> 0	> 0	< 0
	$\frac{\partial T}{\partial v_{\text{deg},\text{c2}}}$				

---

Description	Weight	Desired	Degradation	Activation
12 <i>Cry1</i> knockout period	5	< 95%	92.1%	193.4%
		$\frac{T(Cry1^{-/-})}{T(WT)}$		
13 <i>Cry2</i> knockout period	5	> 115%	131.8%	99.4%
		$\frac{T(Cry2^{-/-})}{T(WT)}$		
14 Fraction CRY1 entering nucleus	1	0.40	0.195	0.059
		$\frac{y_{\max}(CRY1_n)}{y_{\max}(CRY1 + CRY1_n)}$		
15 Fraction CRY2 entering nucleus	1	0.35	0.139	0.059
		$\frac{y_{\max}(CRY2_n)}{y_{\max}(CRY2 + CRY2_n)}$		
16 Time delay between nuclear re- pressors and mRNA	3	75%	0.850	0.848
		$t_{\max}(\text{nuclear protein}) - t_{\max}(\text{mRNA})$		

---

Description	Weight	Desired	Degradation	Activation
17 Time delay between mRNA and cytoplasmic protein	3	25%	0.057	0.095
$t_{\max}(\text{mRNA}) - t_{\max}(\text{protein})$				
18 Time delay between cytoplasmic protein and nuclear protein	3	0%	0.093	0.057
$t_{\max}(\text{protein}) - t_{\max}(\text{nuclear protein})$				

---

### 2.2.3 Model validation and dynamics

The model was validated by comparing the simulated dynamics to experimental measurements. First, the time course plots of the state variables display reasonable phases and amplitudes, and oscillate with a period of 23.7 hours (figure 2.3). The knockout periods are 21.7 hr (91.4% of WT) for  $Cry1^{-/-}$  and 31.5 hr (133% of WT) for  $Cry2^{-/-}$ , indicating that the two feedback loops are indeed redundant with different free-running periods.

#### SiRNA knockdowns

SiRNA knockdowns were performed *in silico* by increasing the degradation rate for the corresponding mRNA; shown in figure 2.4, as done previously in [22].  $Cry1$  and  $Cry2$  knockdowns in wild type conditions show close agreement to experiment [6],

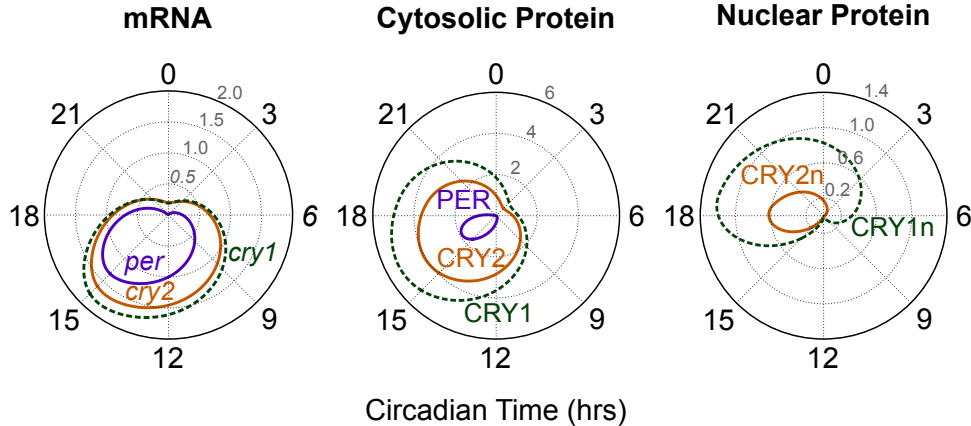


**Figure 2.3: Time Course Plots.** The three polar plots show the time-varying levels of each clock component for optimal parameter set. In these plots, the amplitude of each variable (always positive) is plotted against its phase,  $0 \rightarrow 2\pi$ . Since the limit cycle is periodic, this results in a closed curve. Rising mRNA levels caused by low repressor concentrations (CT12) result in accumulating cytosolic protein (left plot). Lower levels of PER prevent all the available CRY from entering the nucleus (middle plot). High levels of nuclear repressors halt transcription until both CRYs have degraded (right plot).

and demonstrate that altering the nuclear CRY1/CRY2 ratio is effective in changing the period of oscillation.

### CRY2 cytosolic stabilization

The *Dyrk1a* knockdown in [16] serves as another demonstration of the change in period as a response to a change in nuclear CRY1/CRY2 ratio. To demonstrate the effect in silico, the degradation rate of cytosolic CRY2 was decreased. Matching experimental evidence, the cytosolic CRY2 levels rose, with a corresponding change in the nuclear CRY ratio and decrease in period.

### Single cry perturbations

The *Cry1<sup>+/−</sup> Cry2<sup>−/−</sup>* and *Cry1<sup>−/−</sup> Cry2<sup>+/−</sup>* single/double knockout perturbations ([5]) were approximated with an appropriate knockout and siRNA knockdown, and show the correct period shortening. With one *Cry* knocked out, the levels of cyto-

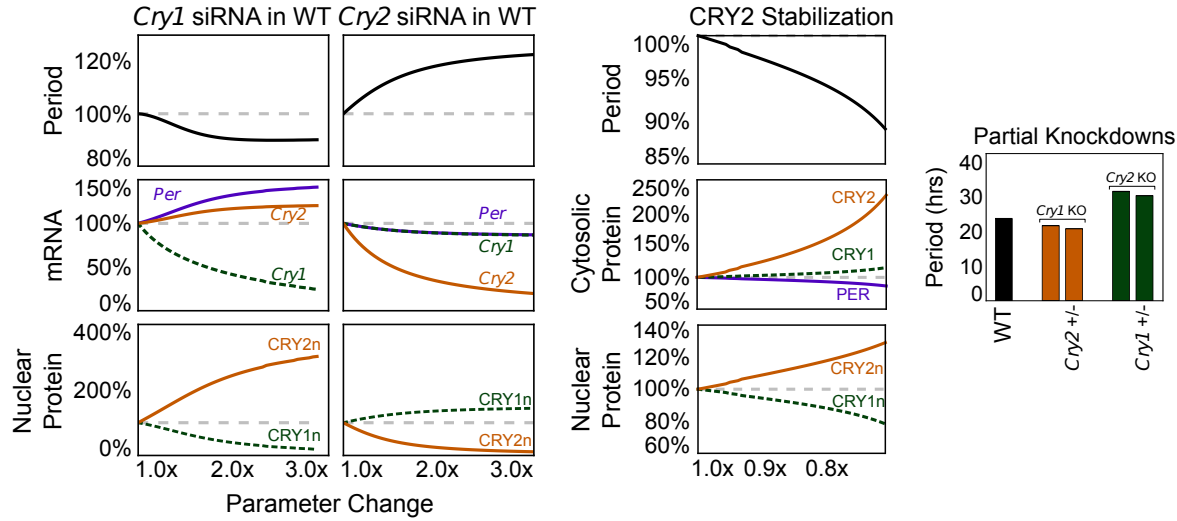


**Figure 2.4: Model Validation.** When comparing against existing experimental results, the model shows the correct response for *Cry1* siRNA, *Cry2* siRNA, and  $CRY_c$  stabilization (left, middle), through an adjustment in the nuclear  $CRY1/CRY2$  ratio. The model also correctly captures the single/double knockout phenotype of [5], (right)

plasmic PER are no longer stoichiometrically limiting. In this case, less *Cry* leads to less nuclear complex, which is cleared faster.

## 2.2.4 Prediction of KL001 mechanism

Using the completed model, I investigated possible mechanisms by which KL001 might lengthen the circadian period. Experimental evidence indicates that stabilization of CRY can either lengthen the period (*Fbxl3* knockdown) or shorten the period (*Dyrk1a* knockdown). Assuming equal effect on both isoforms of *Cry*, the model confirms that cytoplasmic stabilization results in period shortening, since excess CRY expedites the nuclear import of the PER:CRY repressive complex. However, stabilizing nuclear CRY (figure 2.2, last column) yields the appropriate period lengthening observed experimentally. We therefore predicted that KL001 acts primarily in the nucleus, potentially through the FBXL3 degradation pathway. Additionally, the model predicts that the compound's effect on  $Cry1^{-/-}$  and  $Cry2^{-/-}$  systems would be sim-

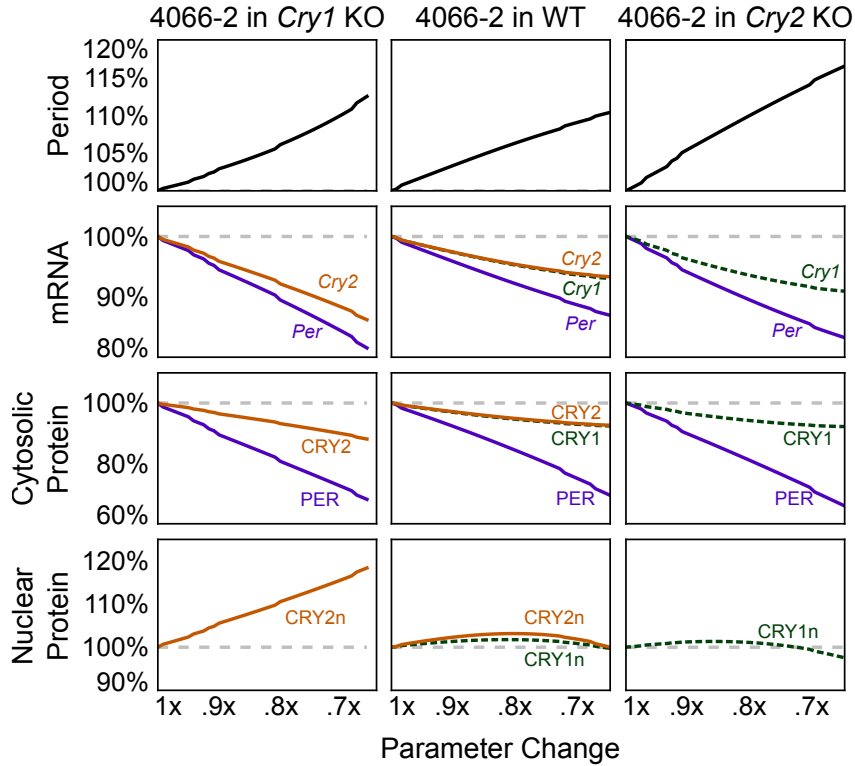


**Figure 2.5: Model Prediction of the KL001 Mechanism.** *In silico* response to equal stabilization of both CRYs in the nucleus results in longer periods (middle column), matching observed results. The model correctly predicts that stabilization of individual CRYs in the knockout environments also causes period lengthening.

ilar to its effect on the wild type clock, causing dose-dependent period lengthening (figure 2.5, left and right).

### Experimental confirmation

Experimental tests of the model's predictions were performed. Nuclear CRY1 and CRY2 levels were up-regulated and almost sustained, respectively, while PER1 level was strongly down-regulated by the compound, supporting stabilization of nuclear CRY, the predicted mechanism. Additionally, continuous treatment with KL001 lengthened the period in both *Cry1* and *Cry2* knockout cells in a dose-dependent manner. Similarly, the compound caused period lengthening in both CRY1 and CRY2 knockdown U2OS cells. We further investigated the effect of KL001 in SCN explants,

which show robust rhythms even in the absence of *Cry1*, due to intercellular coupling [23]. Both *Cry1* and *Cry2* knockout SCN exhibited dose-dependent period lengthening by the compound treatment. Thus, in a single *Cry* knockout, stabilization of either nuclear CRY1 and CRY2 causes period lengthening, confirming model predictions.

## 2.3 Conclusion

### 2.3.1 Insights into Circadian Network Design

Mathematical modeling has revealed how the balancing of two redundant feedback loops can provide fine control over the oscillatory period. A contour plot of period vs CRY1 or CRY2 abundance is shown in figure 2.6, which shows that the model's period is largely insensitive to the total amount of CRY (45° line), but highly dependent on the ratio of the two isoforms. Sensitivity analysis of our mathematical model (figure 2.7) reveals that subtle changes in most of the involved rates can have an effect on the clock's free running period, which could be caused by evolutionary noise. Since many studies have linked entrainment to non-natural periods with long-term health problems, a mechanism to align the clock's natural period to that of the environment would be advantageous. It is therefore possible that the period control afforded by CRY1/CRY2 balancing is a deliberately conserved design principle of the circadian clock, which confers period robustness against random mutations of clock components. Indeed, the presence of independent control of the cytosolic CRY2 levels suggests that the biological clock can control its period through simple post-translational modifications [16].

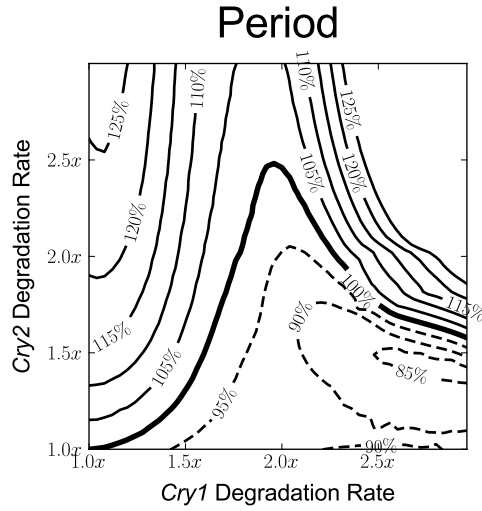


**Figure 2.6: Simultaneous Knockdown of *Cry1* and *Cry2*.** Period contours (% change) resulting from simultaneous *in silico* siRNA knockdowns of *Cry1* (x-axis) and *Cry2* (y-axis). The plot shows that the CRY1/CRY2 ratio determines the period, independent of total CRY, for perturbations up to twice the normal mRNA degradation rate.

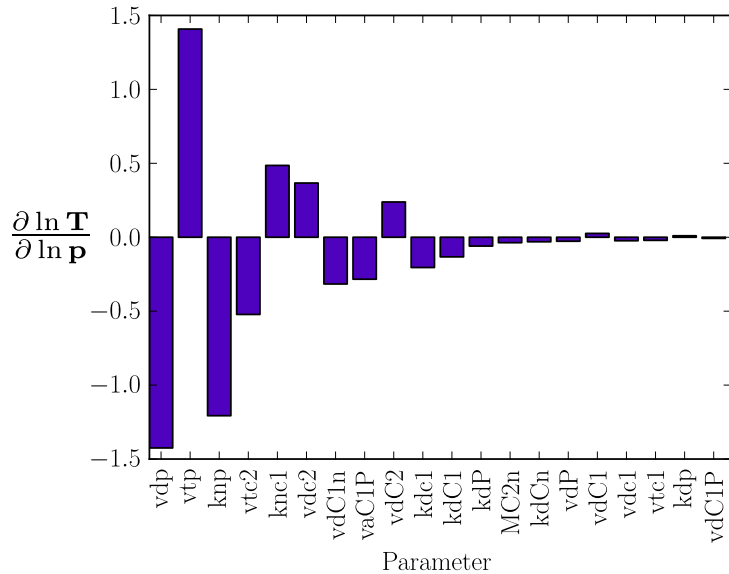


**Figure 2.7: First Order Relative Period Sensitivities.** Dimensionless period sensitivities with respect to the kinetic parameters in the degradation-based model. Perturbations to most clock rates result in noticeable changes to the free-running period. Many of the most sensitive parameters are transcriptional rates, which can be easily changed through mutation of DNA promoter regions.

### 2.3.2 Identifiability of model parameters

Due to the high dimensionality of the model equations and sparsity of the experimental data, it is likely that more than one set of parameters would fit the cost function defined in table 2.4. While the fact that *any* parameter set for the given model equations reproduces experimental results is enough to confirm that our hypothesized mechanism is mathematically consistent, we must be careful in placing too much confidence in predictions based on the particular parameter set generated by the optimization algorithm. While subsequent experimental results confirm many of our model predictions, a more rigorous exploration of parameter space would allow us to determine which predictions are constrained by the available experimental data. However, incorporating error ranges via standard techniques such as bootstrap techniques are infeasible when using a genetic algorithm optimization strategy. In chapter 3, I describe techniques to improve computational efficiency to allow a more systematic evaluation of predictive confidence.

# Chapter 3

## Identifiability analysis for models of circadian rhythms<sup>1</sup>

### 3.1 Background

A cell's behavior is governed by the dynamic and selective expression of its genes, in which each protein's activity depends on a careful balance between transcription, translation, transport, and degradation rates. These rates, which change with environmental conditions and are often impossible to measure accurately *in vivo* or *in vitro*, determine the function of a regulatory pathway. While studying the roles of individual proteins can often provide some insight on how a particular function is achieved, this approach is limited in explaining complicated cellular phenomena at the scale of dozens to hundreds of interacting genes. With the aid of mathematical models, it is increasingly possible to create *in silico* realizations of genetic regulatory networks to examine their dynamic properties. For example, in the previous chapter, I presented a mathematical model of gene regulation for circadian rhythms,

---

<sup>1</sup>Portions of this chapter are published in P. C. St. John and F. J. Doyle, "Estimating confidence intervals in predicted responses for oscillatory biological models.", *BMC Syst. Biol.*, vol. 7, p. 71, July 2013.

using new data from small molecule modulators to gain further insight into clock dynamics.

Essential to understanding how genetic circuits operate is connecting how inputs (i.e., environmental changes, extracellular signals) are processed to give the appropriate outputs (protein expression, cellular response). Models of genetic regulatory networks, often sets of ordinary differential equations (ODEs), contain many unknown parameters that must be estimated from experimental data [24]. Derivatives of the model output with respect to changes in input, known as local sensitivities, are frequently validated experimentally or used to predict potential targets for pharmaceuticals [25]. In chapter 2, I used local sensitivities within the cost function to ensure the model matched previously known experimental results. However, since sensitivities can change drastically with respect to the particular parameter values chosen, the confidence associated with parameter and sensitivity values is an important consideration in model analysis and design.

### 3.1.1 Identifiability analysis

*Practical identifiability analysis* is concerned with calculating confidence intervals in parameter estimates resulting from uncertainty in experimental data [26]. Several techniques for such an analysis currently exist, and are commonly used in analyzing biological models [27, 28, 29]. In one method, the inverse of the Fisher information matrix is used to provide estimates of the variance in each parameter. However, since this method assumes a linearized model, the resulting symmetric normal distributions for each parameter do not accurately reflect the mapping of nonlinear models [30]. In the bootstrap method, distributions in parameter estimates are found through optimum fits to repeated physical or *in silico* measurements. While accurate in finding the true nonlinear confidence intervals, this approach requires efficient and robust parameter estimation convergence.

## **Difficulties imposed by periodic systems**

In periodic systems, such as the models examined in this thesis, the behavior (and existence) of limit cycle oscillations is a discontinuous function of the parameters. Optimal values are traditionally found through trial-and-error type approaches [10, 12] or genetic algorithm search strategies [11], both of which are not amenable to bootstrap methods. Additionally, since the solutions are oscillatory, additional care must be taken in the calculation of the first-order sensitivity values. In this chapter, we calculate the sensitivity of the oscillatory period to parameter perturbation, a biologically relevant quantity that is often measured experimentally [21]. Due to these complications, rigorous identifiability analyses of these models are typically not performed.

In this chapter, a bootstrap uncertainty analysis appropriate for oscillatory biological models is developed and applied to the model of circadian rhythms described in chapter 2 [3]. These networks serve as an excellent example of a functional genetic circuit, able to process subtle environmental cues while remaining robust to temperature variations and evolutionary disturbances. Accurate limit cycle models must capture not only the correct time-dependent dynamics, but also the correct input-output response. For circadian rhythms, high-throughput microarrays have provided high-resolution time-series data of gene expression levels [31]. Additionally, knockdown experiments using RNA interference technology (siRNA) and small molecule modulators have resulted in a wealth of data on the dynamic responses to changes in key rates [3, 6, 32, 33]. This data, together with qualitative knowledge of the underlying network structure, permits the use and verification of a suitable uncertainty analysis.

### Alternative parameter estimation methods

To enable a bootstrap approach, we employ an efficient parameter estimation routine optimized for limit cycle models. Motivated by the increasing availability of high-resolution time-series measurements, we use an approach similar to multiple shooting, in which a nonlinear and discontinuous parameter estimation problem is transformed into a high-dimensional yet local optimization and solved via nonlinear programming [34]. Since the desired shape of the limit cycle solution is known *a priori*, a relatively accurate initial guess for the parameters and trajectories can be found. By using multiple sets of *in silico* data of varying quality, we illustrate how error in experimental results is propagated to uncertainty in parameter sensitivity. Lower quality data - with either higher error or fewer sampling points - result in wider distributions of limit cycles and less identifiable responses. These results can be used in *a priori* experimental design, finding the minimum sampling points needed for an estimated experimental error to enable accurate modeling. Additionally, we show using literature data how this method can be used to discriminate between candidate model structures, revealing which one yields the highest predictive confidence.

## 3.2 Methods

### 3.2.1 Collocation Methods

The estimation of the unknown kinetic parameters is accomplished via nonlinear programming [34]. In this method, we divide the limit cycle trajectory  $\mathbf{x}(t, \mathbf{p})$  into  $\mathcal{N}$  finite elements of length  $h$ , and approximate each with a  $\mathcal{K}$  degree Lagrange interpolating polynomial,  $\mathbf{x}_i^{\mathcal{K}}(t)$ , using an internal time  $\tau \in [0, 1]$ . For finite element

*i*:

$$\begin{aligned}
 t &= h(i + \tau) \\
 \ell_j(\tau) &= \prod_{k=0, k \neq j}^{\mathcal{K}} \frac{\tau - \tau_k}{\tau_j - \tau_k} \\
 \mathbf{x}_i^{\mathcal{K}}(\tau) &= \sum_{j=0}^{\mathcal{K}} \ell_j(\tau) \mathbf{x}_{ij}.
 \end{aligned} \tag{3.1}$$

We also ensure that the interpolating polynomial matches system dynamics at each collocation point,  $\tau_k$ , by setting

$$\sum_{j=0}^{\mathcal{K}} \mathbf{x}_{ij} \frac{d\ell_j(\tau_k)}{d\tau} = h\mathbf{f}(\mathbf{x}_{ij}, \mathbf{p}) \tag{3.2}$$

for  $k = 1, \dots, \mathcal{K}$ .

Additionally, the interpolating polynomials for each finite element must form a continuous function, so the following continuity constraints are imposed:

$$\mathbf{x}_{i+1,0} = \sum_{j=0}^{\mathcal{K}} \ell_j(1) \mathbf{x}_{i,j} \tag{3.3}$$

for  $i = 1, \dots, \mathcal{N} - 1$ .

Periodic conditions are imposed by setting the beginning of the first element equal to the end of the final element:

$$\mathbf{x}_{0,0} = \sum_{j=0}^{\mathcal{K}} \ell_j(1) \mathbf{x}_{\mathcal{N},j} \tag{3.4}$$

The  $\tau_k$  values are chosen for optimal accuracy, here we use Gauss-Radau roots so that the resulting method has stiff decay [34]. With  $\mathcal{K} = 5$ :

$$\tau = \{0.000, 0.057, 0.277, 0.584, 0.860, 1.000\}$$

The interpolating polynomials can now be compared to the experimental data. For each measured value,  $\hat{\mathbf{x}}(t_n)$ , the corresponding simulated values  $\mathbf{x}^K(t_n)$  can be interpolated from  $\mathbf{x}_{ij}$ :

$$\mathbf{x}^K(t_n) = \sum_{j=0}^K \ell_j(\tau_n) \mathbf{x}_{ij} \quad (3.5)$$

$$\text{for } n = 1, \dots, \mathcal{M}$$

where  $i$  and  $\tau_n$  are selected for the appropriate finite element and sampling time. The objective function  $\Phi(\mathbf{x}, \mathbf{p})$  is thus:

$$\Phi(\mathbf{x}, \mathbf{p}) = \sum_n^{\mathcal{M}} \left( \frac{\mathbf{x}^K(t_n) - \hat{\mathbf{x}}(t_n)}{\mathbf{\sigma}_n} \right)^2 \quad (3.6)$$

where  $\mathbf{\sigma}_n$  is the measurement error associated with measurement  $n$ . Since  $\mathbf{x}$  and  $\mathbf{\sigma}$  are vectors, the division in equation (3.6) must be performed element-wise. This cost function was taken from a similar multiple-shooting approach to parameter estimation [35].

Since the cost function (equation (3.6)) and equality constraints (equation (3.2), equation (3.3), and equation (3.4)) now satisfy continuity and differentiability requirements [36], parameter estimation can now be accomplished via constrained nonlinear programming (NLP) instead of a global search strategy. The solution is subject to variable bounds:

$$\mathbf{x}_{LB} \leq \mathbf{x} \leq \mathbf{x}_{UB} \quad (3.7)$$

$$\mathbf{p}_{LB} \leq \mathbf{p} \leq \mathbf{p}_{UB}$$

The numerical implementation is accomplished using IPOPT [37], using the MA57 [38] linear solver. The CasADi computer algebra package [39] was used to provide an interface to the IPOPT numerical libraries and supply derivatives to the cost and equality function calls through automatic differentiation.

### 3.2.2 Generating Initial Values

Solution of the NLP described in section 3.2.1 requires a suitable initial guess for the optimal state profiles,  $\mathbf{x}^*$ , and kinetic parameters,  $\mathbf{p}^*$ . To find approximate values for these variables, a smoothed periodic B-spline,  $\tilde{\mathbf{x}}$ , is found using experimental data for each state variable using SciPy's interpolate module [40]. Initial values for  $x_{ij}$  are obtained by evaluating this spline at each  $\tau_k$  for each finite element.

$$\mathbf{x}_{ij}^* \approx \tilde{\mathbf{x}}(t_{ij})$$

where  $t_{ij} = h(i - 1 + \tau_j)$  (3.8)

for  $i = \{1, \dots, \mathcal{N}\}, j = \{1, \dots, \mathcal{K}\}$

Since

$$\frac{d\tilde{\mathbf{x}}}{dt} \approx \mathbf{f}(\tilde{\mathbf{x}}, \mathbf{p}), \quad (3.9)$$

approximate values for  $\mathbf{p}$  can be obtained by solving the simpler unconstrained NLP,

$$\min_{\mathbf{p}} \sum_i^{\mathcal{N}} \sum_j^{\mathcal{K}} \left( \frac{d\tilde{\mathbf{x}}(t_{ij})}{dt} - \mathbf{f}(\tilde{\mathbf{x}}(t_{ij}), \mathbf{p}) \right)^2 \quad (3.10)$$

in which  $t_{ij}$  is the same as in 3.8 and the bounds on  $p$  are the same as in equation (3.7).

### 3.2.3 First Order Sensitivity Analysis

After determining an optimal parameter set for the given experimental data, relevant first order sensitivity coefficients for oscillatory models are found using the procedure from [21], summarized here. First, initial conditions and oscillatory period are verified by solving the boundary value problem (BVP):

$$\min_{\mathbf{x}(0), T} \begin{pmatrix} \mathbf{x}(T) - \mathbf{x}(0) \\ \dot{\mathbf{x}}_0(0) \end{pmatrix} \quad (3.11)$$

where  $\dot{\mathbf{x}}_0(0)$  denotes the time-derivative of the first state variable, evaluated at  $t = 0$ . This BVP is solved using Newton's method, employing the SUNDIALS packages CVODES for ODE integration and KINSOL for the Newton iterations [20].

Time-dependent parametric sensitivities,

$$\mathbf{S}(t) \equiv \frac{\partial \mathbf{x}(t)}{\partial \mathbf{p}}, \quad (3.12)$$

are obtained by using the staggered-direct method from the CVODES integrator [41]. Sensitivities of the period,  $\frac{\partial T}{\partial \mathbf{p}}$ , can be obtained directly from sensitivities integrated for one pass of the limit cycle (see [21] or [42] for further details) through a linear solve:

$$\begin{bmatrix} \mathbf{M} - \mathbf{I} & \dot{\mathbf{x}}(T) \\ \frac{\partial \mathbf{f}_0}{\partial \mathbf{x}}(\mathbf{x}(0)) & 0 \end{bmatrix} \begin{bmatrix} \vdots \\ \frac{\partial T}{\partial \mathbf{p}} \end{bmatrix} = \begin{bmatrix} -\mathbf{S}(T) \\ -\frac{\partial \mathbf{f}}{\partial \mathbf{p}}(\mathbf{x}(0)) \end{bmatrix} \quad (3.13)$$

in which  $\mathbf{M}$  is the Monodromy matrix,  $\mathbf{I}$  is the identity matrix, and the unknown vector contains the relevant period sensitivities.

Since parameter values often span several orders of magnitude, an often more useful measure is the relative period sensitivity, which is independent of the magnitude of the period or parameter value.

$$\frac{\partial \ln T}{\partial \ln \mathbf{p}} = \frac{\mathbf{p}}{T} \frac{\partial T}{\partial \mathbf{p}} = \frac{\partial T}{T} \Big/ \frac{\partial \mathbf{p}}{\mathbf{p}} \quad (3.14)$$

Thus, a relative period sensitivity of 1 indicates that a 1% increase in the parameter value will result in a 1% increase in the period.

### 3.2.4 Generation of data for bootstrap methods

For each run, two thousand simulated measurements,  $\hat{x}_i(t_j)$ , were generated from the true data,  $\tilde{x}_i(t_j)$ , using a normal distribution with  $\mu = \tilde{x}_i(t_j)$  and  $\sigma_{ij} = \xi \tilde{x}_i(t_j) +$

$\eta \max_j \tilde{x}_i(t_j)$ , in which  $\xi$  is the relative and  $\eta$  is the absolute error. Each simulated data set was then used to find a unique optimum parameter set,  $\mathbf{p}^*$ . Data sets that failed to converge, or reached a steady state solution (in which periodic sensitivities are undefined), were discarded from further analysis.

For the *in silico* data of varying quality used in figures 3.2-3.4, we used the known limit cycle  $\mathbf{x}(t)$  to generate data points  $\hat{x}_i(t_j)$  at each of  $\mathcal{M}$  sampling points. The effect of increasing error and decreasing number sampling points were tested independently:

$$\xi = \{.01, .05, .10, .20, .30\}; \quad \mathcal{M} = 20$$

$$\mathcal{M} = \{30, 20, 15, 10, 5\}; \quad \xi = 0.15$$

Since standard deviations in the data distributions were also used as optimization weights, a small amount of absolute error ( $\eta = 0.001$ ) was added to ensure errors in small values did not dominate the cost function.

### 3.2.5 Calculation Times

Each parameter estimation took approximately 4 seconds on a 2.53GHz processor, with the subsequent limit cycle solution integration and sensitivity calculation taking approximately 0.5 seconds. Due to the parallel nature of the 2000 trials, computation times were alleviated by distributing the tasks onto a cluster of 160 compute nodes.

### 3.3 Results and discussion

Mechanistic models of biological processes are often posed as nonlinear, time-invariant systems of ordinary differential equations (ODEs) [10, 11, 12], of the form:

$$\frac{d\mathbf{x}}{dt} = \mathbf{f}(\mathbf{x}(t), \mathbf{p}) \quad (3.15)$$

in which the vector of state variables  $\mathbf{x}(t)$  describe the time-dependent activity of important species (i.e., mRNA, proteins, or metabolites), the parameters  $\mathbf{p}$  are the kinetic rate constants, and the vector function  $\mathbf{f}(\mathbf{x}(t), \mathbf{p})$  contains the transcription, translation, transport, and degradation rate laws of the gene regulatory network. In modeling rhythmic phenomena, we typically seek models and parameter values that display *limit cycle* oscillations - where for the solution approaches a non-trivial periodic trajectory:

$$\lim_{t \rightarrow \infty} \mathbf{x}(t) = \mathbf{x}(t + T). \quad (3.16)$$

Here the period of oscillation is the smallest  $T > 0$  in which equation (3.16) holds. Limit cycle oscillations are independent of the system's initial values  $\mathbf{x}(0)$ , and are instead determined completely by the parameters  $\mathbf{p}$ .

Experimental values for  $\mathbf{p}$  are rarely available. Given time-series experimental measurements  $\hat{x}_i(t_j)$  for each state variable in a limit cycle system, we find optimal parameters  $\mathbf{p}^*$  such that the error between the experimental measurements and the simulated limit cycle is minimized [35]:,

$$\mathbf{p}^* := \arg \min_{\mathbf{p}} \sum_i^{states} \sum_j^{data} \frac{(\hat{x}_i(t_j) - x_i(t_j, \mathbf{p}))^2}{\sigma_{ij}^2}. \quad (3.17)$$

Here  $\sigma_{ij}$  is the standard deviation associated with the measured mean of state  $i$  at time  $j$ . Using the data points  $\hat{x}_i(t_j)$  to generate a suitable initial guess, parameter estimation may proceed via a nonlinear programming approach as described in 3.2.

In this chapter, we assume that all states are measured to demonstrate how initial guesses can be generated directly from the input data. However, for systems with unmeasured states, initial guesses for the trajectory and parameter values can be provided by another approach, such as a global optimization routine. A bootstrap method was implemented by repeatedly sampling input data distributions to calculate a population of optimal parameter fits.

After finding optimal parameter fits, we used the models to predict how perturbations change systems dynamics by performing a first order sensitivity analysis. Since adjustments to periodic systems in response to inputs are often manifested through temporary changes in oscillatory period, relative period sensitivities,

$$\frac{\partial \ln T}{\partial \ln p} \quad (3.18)$$

were calculated due to their independence of parameter magnitude [21, 42, 43]. Relative period sensitivities were integrated into the bootstrap method by calculating appropriate sensitivities for each estimated parameter set.

Of particular importance in determining the reliability of a model prediction is whether an output response maintains a consistent direction despite noise in measurement data. We therefore define a sensitivity value to be practically identifiable for given input data if 95% of the distribution maintains a consistent sign, similar to definitions for parameter identifiability used in previous studies [30, 44]. An overview of the method is shown in figure 3.1.

### 3.3.1 Effect of data quality on predictive confidence

We first analyze the degree to which uncertainty in input data is propagated to uncertainty in output predictions. To achieve this, we generate *in silico* data from a previously published model of circadian rhythms, using relative error  $\xi$  to generate

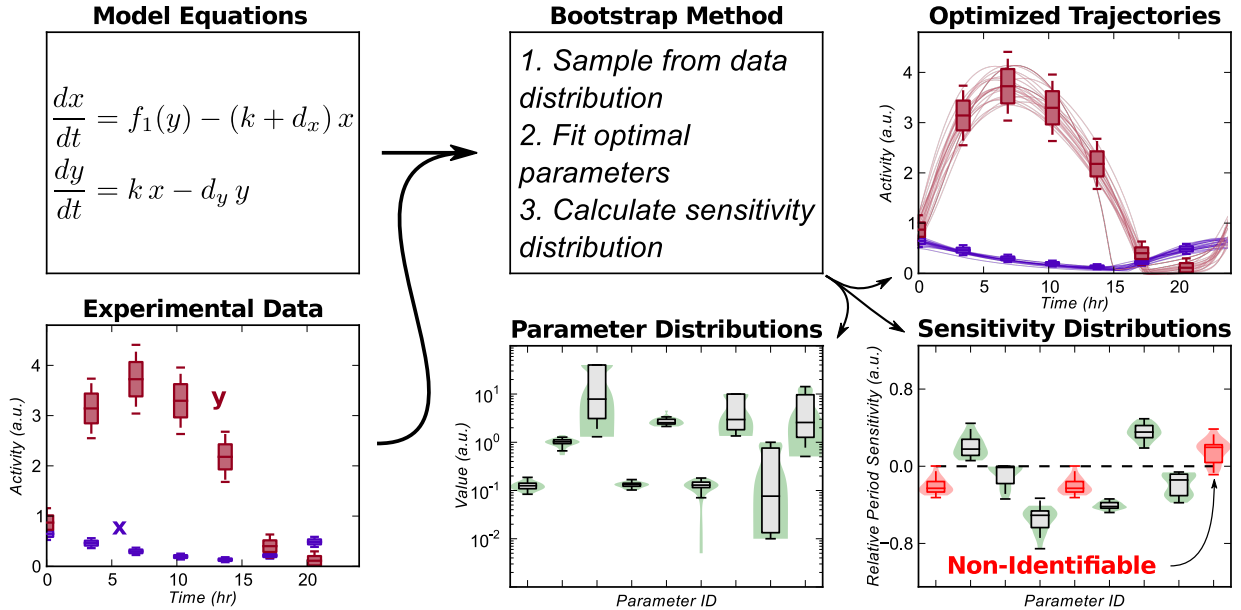


**Figure 3.1: Parameter estimation and bootstrap methods flowchart.** The demonstrated method calculates confidence intervals in the sensitivity of limit cycle models. An oscillatory model and experimental (or simulated) data are inputs to the bootstrap method. Unique data sets are then used to calculate optimum limit cycle trajectories. The resulting distribution in sensitivities highlight whether a particular response is identifiable (i.e., consistent across the majority of bootstrap trials.)

normally distributed data ( $\sigma_{ij} = \xi \hat{x}_i(t_j)$ ) at each of  $\mathcal{M}$  sampling points. As expected, solution trajectories drifted further from the nominal limit cycle for higher values of error,  $\xi$ , or lower sampling density,  $\mathcal{M}$ , (figure 3.2). However, the overall shape of the oscillatory profiles remained relatively similar, even for rather high  $\xi$  or low  $\mathcal{M}$ .

Figure 3.3 shows violin plots of the probability distribution for each parameter set and corresponding sensitivity evaluation for increasing  $\xi$ , while figure 3.4 shows similar plots for decreasing  $\mathcal{M}$ . Interestingly, there is little correlation between the identifiability of a parameter and its corresponding sensitivity value. For example,  $v_{dP}$ , the maximum degradation rate of Per mRNA, shows a very tight clustering about its nominal parameter value, while the sensitivity of this parameter loses identifiability for even small values of  $\xi$ . Conversely,  $K_{dCn}$ , the Michealis-Menten constant associated with the degradation of nuclear CRY, shows large variations in possible

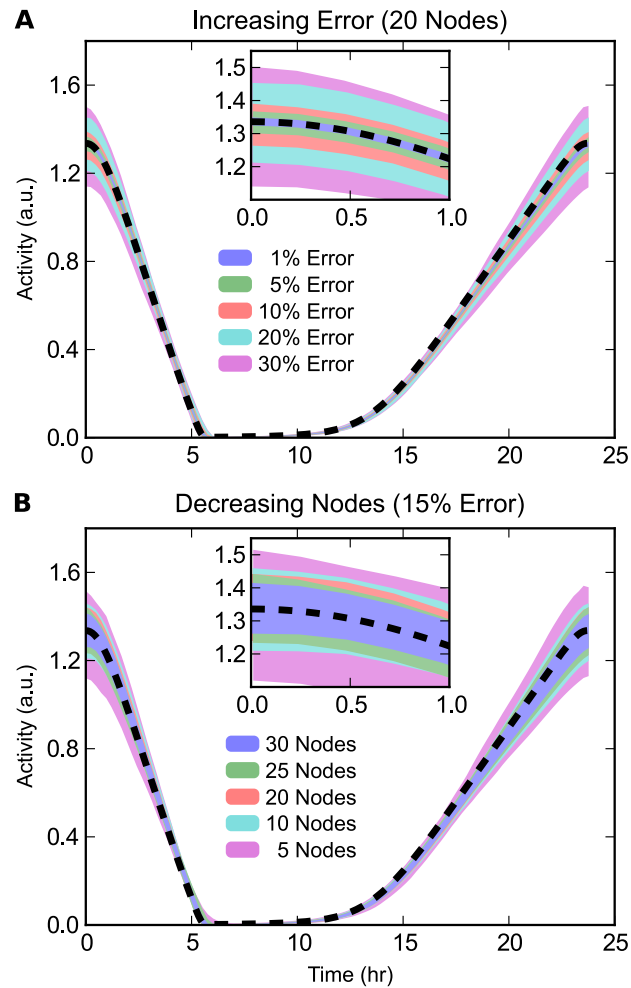


**Figure 3.2: Time-course Profiles of the State Trajectories for Per mRNA.**  
 (A) Increasing relative error,  $\xi$ , with  $\mathcal{M} = 20$ . Possible state variable values are shown as shaded regions, obtained by filling between the 5<sup>th</sup> and 95<sup>th</sup> percentile for values at each time for 2000 independent parameter estimations. Increasing  $\xi$  results in larger deviations from the original model trajectory, shown as a dashed black line.  
 (B) Decreasing number of measurement points,  $\mathcal{M}$ , each with  $\xi = 0.15$ . Higher  $\mathcal{M}$  results in trajectories closer to the true trajectory.

parameter values. However, the period sensitivity of KdCn, despite lying close to the x-axis, remains identifiable, indicating a robust prediction. These results reveal which model responses are constrained by the structure and dynamics of the limit cycle oscillations, and which are dependent on the particular parameterization chosen.

Sensitivities that are experimentally distinguishable from zero are the most important for validation. Calculating a typical experimental value for a relative period sensitivity helps to calibrate which sensitivities might be verified experimentally. Referring to a recent RNA interference screen, periods changes of approximately 1 hour ( 5%) can be reliably measured using luminescence recordings [6]. Assuming an increase in the corresponding mRNA degradation parameter value of 50%, this translates to a relative period sensitivity of 0.1. Thus, many of the identifiable values shown in figures 3.3-3.4 fall within the experimentally measurable range.

### 3.3.2 Application to literature data for model discrimination

We next apply the method to literature time-course data for core clock components [13]. When modeling a genetic regulatory network, many candidate model equations are often considered. We show that a bootstrap uncertainty analysis can also be useful in discriminating between potential model structures based on predictive confidence. Here two variations of the same model are fit: The first model (table 2.1) was originally optimized using a genetic algorithm approach, and thus contains a minimal number of parameters to reduce optimization complexity. The second model (table 3.1) considered contains independent parameters for each rate expression, increasing the number of parameters from 23 to 35.

The literature data used consisted of 7-8 concentration time points across a 24 hour period. Confidence intervals in the data were not available, so an optimistic 3% relative and 0.5% absolute error was assumed for each data point ( $\sigma_{ij} = 0.03 \hat{x}_i(t_j) +$

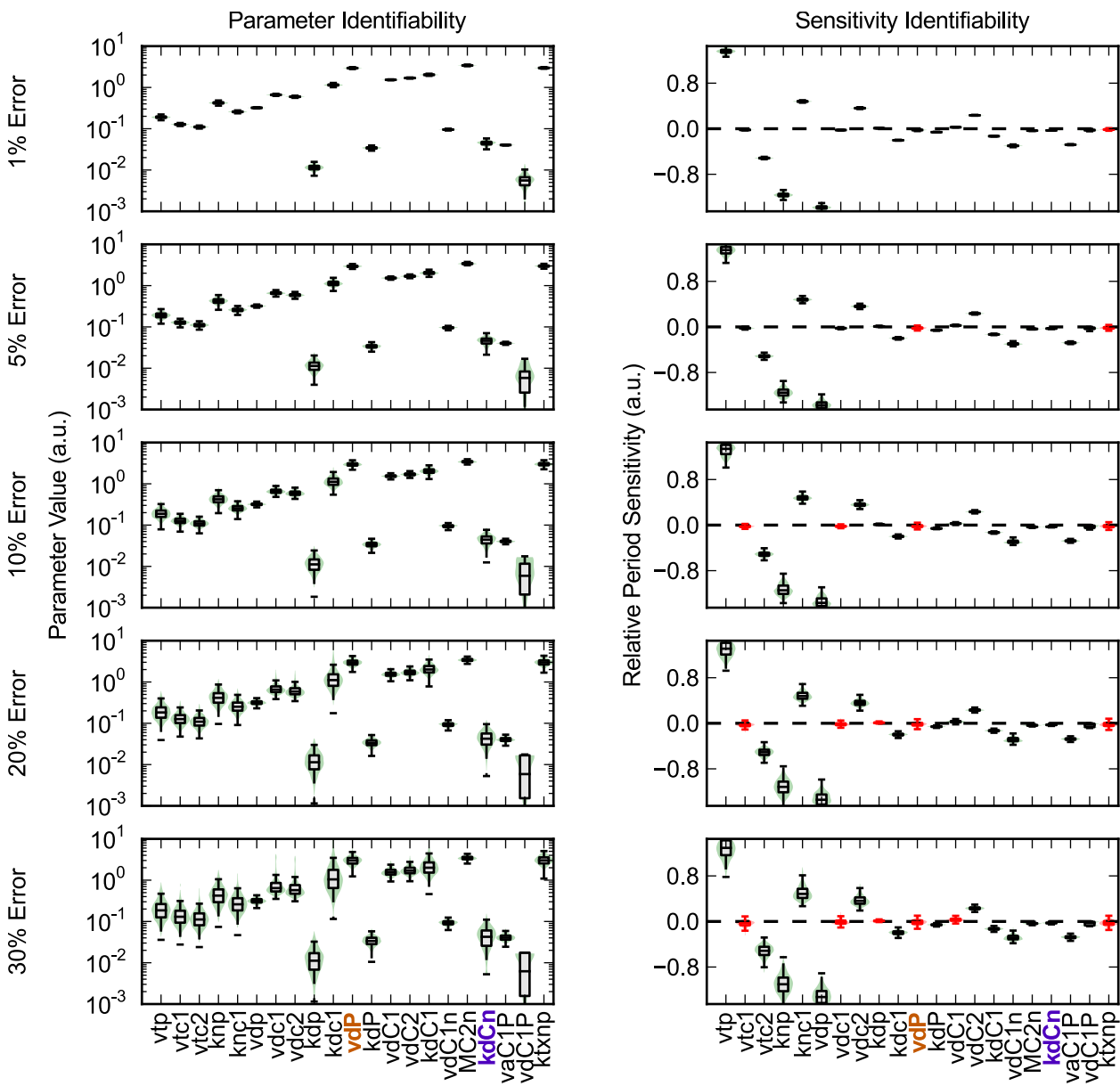


**Figure 3.3: Parameter and Sensitivity Identifiability for Increasing Error.** Increasing  $\zeta$  results in a corresponding decrease in the confidence of the parameter and sensitivity estimates. Violin plots of the parameter values (left) and relative period sensitivities (right) show the distribution of values from each parameter estimation. In the plots, a box plot is superimposed above a kernel density plot to convey the distribution of values. The whiskers used extend to the most extreme data point within 1.5x the inner quartile range. Sensitivities in which the 5<sup>th</sup> and 95<sup>th</sup> percentile values span the x-axis are deemed non-identifiable (red), as the model's response direction can not be accurately estimated. Higher  $\zeta$  also results in wider parameter distributions.

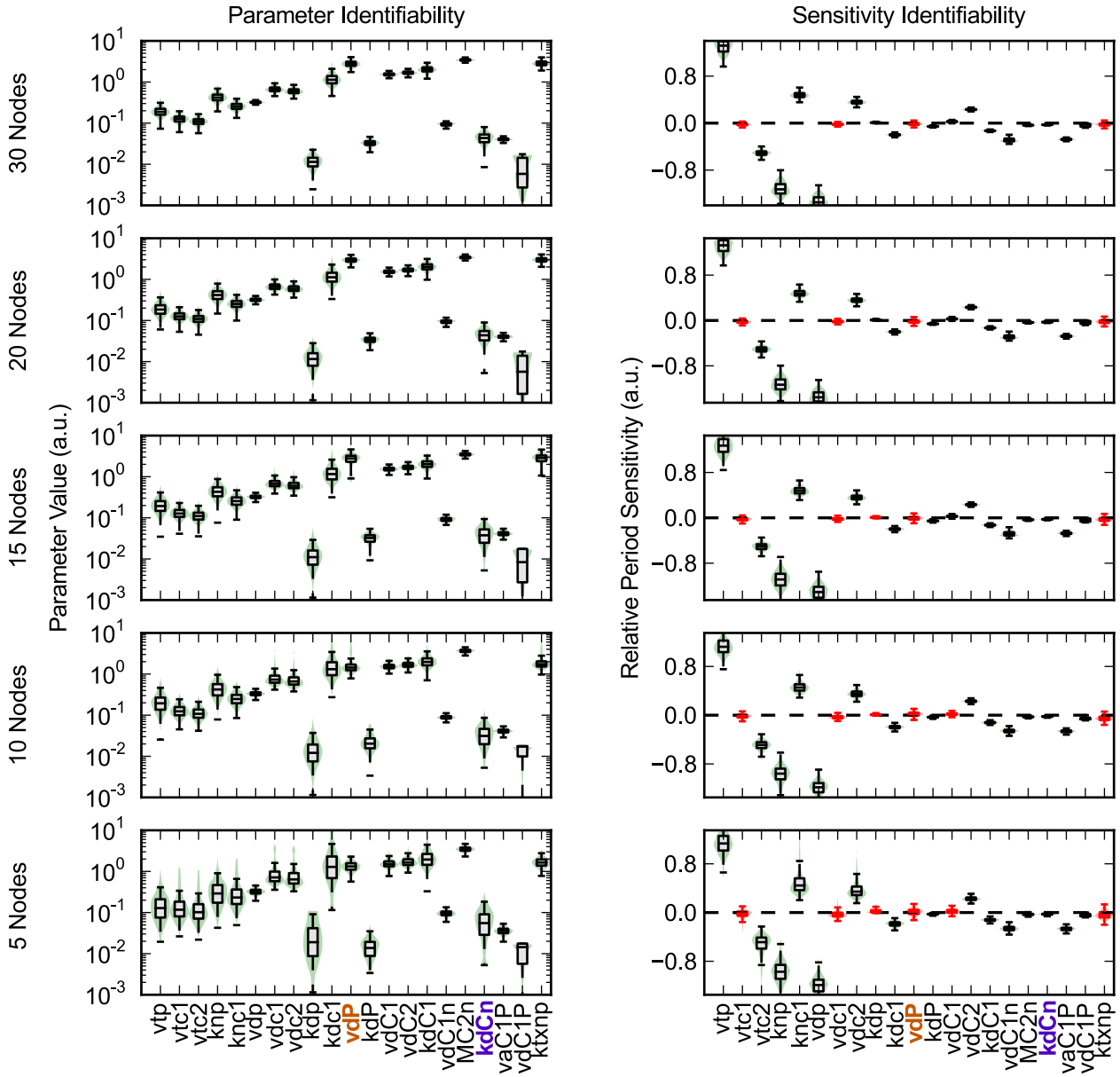


**Figure 3.4: Effect of High-resolution Sampling on Identifiability.** Lower values of  $\mathcal{M}$  result in less constrained parameter and sensitivity values. Similar to figure 3.3, violin plots of the parameters (left) and sensitivities (right) show the distribution from each parameter estimation for decreasing  $\mathcal{M}$ . These results highlight the importance of high-resolution time sampling in generating sensitivity information for oscillatory models.

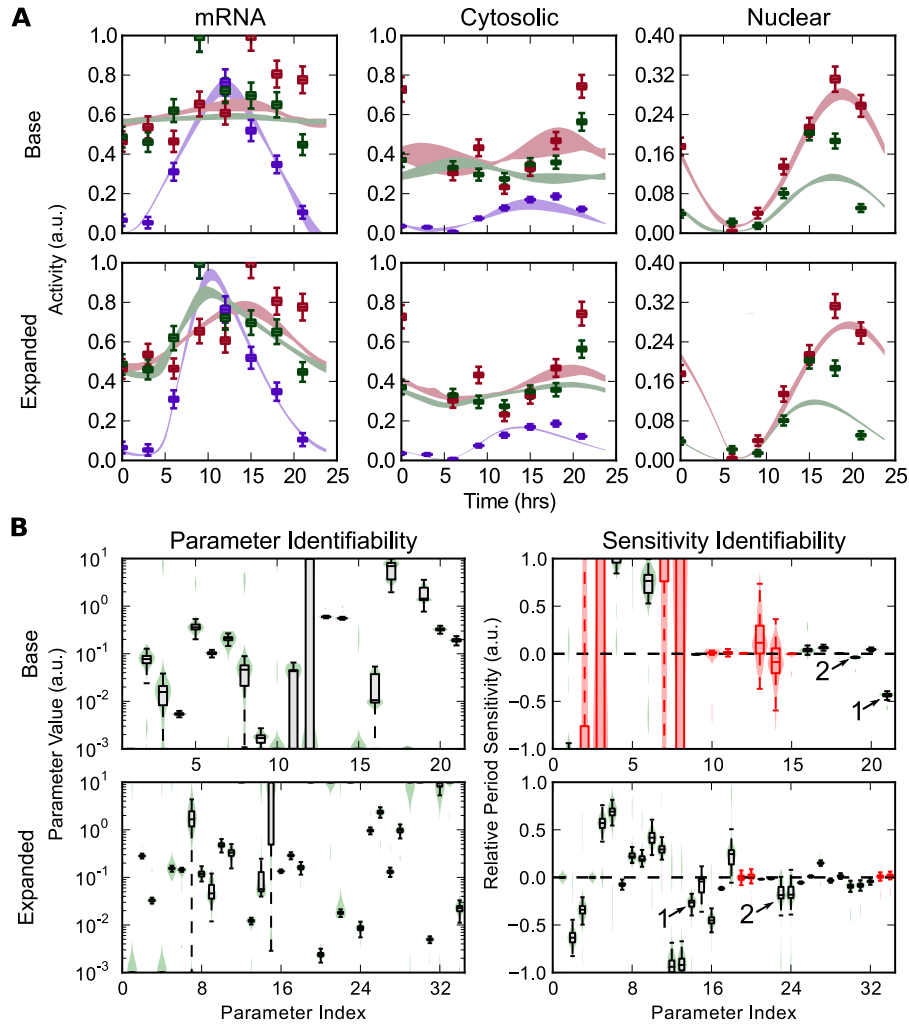


**Figure 3.5: Identifiability Comparison of Two Model Structures.** (A) Bootstrap parameter estimations on two model structures using literature time-series data with estimated errors (box plots). Resulting regions of model trajectories are shaded between the 5<sup>th</sup> and 95<sup>th</sup> percentile. *Per* species are shown in purple, *Cry1* in red, and *Cry2* in green. While both models were able to approximately reproduce the same dynamic response, the expanded model was better able to capture differences between the *Cry1* and *Cry2* profiles. (B) Parameter and sensitivity identifiability for the base and expanded models. Violin plots show the parameter and sensitivity distributions, with unidentifiable sensitivities (90% confidence level) highlighted in red. Despite containing more parameters, the expanded model shows better parameter identifiability and higher confidence in its predicted sensitivities. The PER translation rate (1) and PER-CRY association rate (2) sensitivities are consistent across model equations and are highlighted.

**Table 3.1: Model Equations for the Expanded Model.** These equations have similar reaction stoichiometry to those in table 2.1, but with more parametric degrees of freedom. This model showed better time-series performance than the more constrained model when fit to time-series data.

$$\begin{aligned}
 \frac{d\mathbf{p}}{dt} &= \frac{Vm_1}{1 + Vm_1 \left( \frac{\mathbf{C1N} + \mathbf{C2N} M_1}{K_{i_1}} \right)^3} - \frac{k_1 \mathbf{p}}{1 + \frac{\mathbf{p}}{Km_1}} \\
 \frac{d\mathbf{c1}}{dt} &= \frac{Vm_2}{1 + Vm_2 \left( \frac{\mathbf{C1N} + \mathbf{C2N} M_2}{K_{i_2}} \right)^3} - \frac{k_2 \mathbf{c1}}{1 + \frac{\mathbf{c1}}{Km_2}} \\
 \frac{d\mathbf{c2}}{dt} &= \frac{Vm_3}{1 + Vm_3 \left( \frac{\mathbf{C1N} + \mathbf{C2N} M_3}{K_{i_3}} \right)^3} - \frac{k_3 \mathbf{c2}}{1 + \frac{\mathbf{c2}}{Km_3}} \\
 \frac{d\mathbf{P}}{dt} &= k_4 \mathbf{p} + k_{12} \mathbf{C1N} + k_{13} \mathbf{C2N} - \frac{k_7 \mathbf{P}}{1 + \frac{\mathbf{P}}{Km_4}} - k_{10} \mathbf{P} \mathbf{C1} - k_{11} \mathbf{P} \mathbf{C2} \\
 \frac{d\mathbf{C1}}{dt} &= k_5 \mathbf{c1} + k_{12} \mathbf{C1N} - \frac{k_8 \mathbf{C1}}{1 + \frac{\mathbf{C1}}{Km_5}} - k_{10} \mathbf{P} \mathbf{C1} \\
 \frac{d\mathbf{C2}}{dt} &= k_6 \mathbf{c2} + k_{13} \mathbf{C2N} - \frac{k_9 \mathbf{C2}}{1 + \frac{\mathbf{C2}}{Km_6}} - k_{11} \mathbf{P} \mathbf{C2} \\
 \frac{d\mathbf{C1N}}{dt} &= k_{10} \mathbf{P} \mathbf{C1} - k_{12} \mathbf{C1N} - \frac{k_{14} \mathbf{C1N}}{1 + \frac{\mathbf{C1N} + \mathbf{C2N} M_4}{Km_7}} \\
 \frac{d\mathbf{C2N}}{dt} &= k_{11} \mathbf{P} \mathbf{C2} - k_{13} \mathbf{C2N} - \frac{k_{15} \mathbf{C2N}}{1 + \frac{\mathbf{C1N} + \mathbf{C2N} M_5}{Km_8}}
 \end{aligned}$$

0.005  $\max(\hat{x}_i)$ ). Figure 3.5A shows the resulting time-series profiles for bootstrap estimations of each model. While additional kinetic parameters are typically thought to lower the predictive confidence of a model (the ‘curse of dimensionality’), the expanded model is able to better capture the oscillatory profiles with lower variability between solutions. Parameter and sensitivity distributions, figure 3.5B, similarly show how the expanded model parameterization is able to generate more confident predictions in model response. Since the resulting sensitivity identifiability for both models was relatively poor, we highlight sensitivities which pass a 90% confidence level threshold. These results thus indicate higher-resolution data on circadian com-

**Table 3.2: Parameter Set for Expanded Model.** Parameters for model described in table 3.1, fit to time-series data via nonlinear programming.

	Parameter	Description	Value
1	$M_1$	$Per/CRY2$ activity coefficient	3.632
2	$Vm_1$	$Per$ transcription rate	$9.957 \times 10^{-1}$
3	$Ki_1$	$Per/CRY$ inhibition coefficient	$1.054 \times 10^{-1}$
4	$M_2$	$Cry1/CRY2$ activity coefficient	$1.000 \times 10^{-3}$
5	$Vm_2$	$Cry1$ transcription rate	$2.262 \times 10^{-1}$
6	$Ki_2$	$Cry1/CRY$ inhibition coefficient	$2.049 \times 10^{-1}$
7	$M_3$	$Cry2/CRY2$ activity coefficient	$1.000 \times 10^1$
8	$Vm_3$	$Cry2$ transcription rate	$1.850 \times 10^{-1}$
9	$Ki_3$	$Cry2/CRY$ inhibition coefficient	$1.427 \times 10^{-1}$
10	$k_1$	$Per$ degradation rate	$2.920 \times 10^{-1}$
11	$Km_1$	$Per$ degradation self-inhibition	$6.609 \times 10^{-1}$
12	$k_2$	$Cry1$ degradation rate	$1.000 \times 10^1$
13	$Km_2$	$Cry1$ degradation self-inhibition	$1.823 \times 10^{-2}$
14	$k_3$	$Cry2$ degradation rate	$4.711 \times 10^{-2}$
15	$Km_3$	$Cry2$ degradation self-inhibition	$1.000 \times 10^1$
16	$k_4$	$Per$ translation rate	$1.132 \times 10^{-1}$
17	$k_5$	$Cry1$ translation rate	$3.409 \times 10^{-1}$
18	$k_6$	$Cry2$ translation rate	$1.961 \times 10^{-1}$
19	$k_7$	PER degradation rate	$1.000 \times 10^1$
20	$Km_4$	PER degradation self-inhibition	$1.911 \times 10^{-3}$
21	$k_8$	CRY1 degradation rate	$1.000 \times 10^1$
22	$Km_5$	CRY1 degradation self-inhibition	$2.077 \times 10^{-2}$
23	$k_9$	CRY2 degradation rate	$1.000 \times 10^1$
24	$Km_6$	CRY2 degradation self-inhibition	$1.180 \times 10^{-2}$
25	$k_{10}$	C1N association rate	$5.022 \times 10^{-1}$
26	$k_{11}$	C2N association rate	1.035
27	$k_{12}$	C1N dissociation rate	$1.000 \times 10^{-3}$
28	$k_{13}$	C2N dissociation rate	$2.070 \times 10^{-1}$
29	$M_4$	CRY1n/CRY2n activity coefficient	$1.000 \times 10^1$
30	$k_{14}$	CRY1N degradation rate	$1.000 \times 10^1$
31	$Km_7$	CRY1n degradation inhibition	$5.206 \times 10^{-3}$
32	$M_5$	CRY2n/CRY2n activity coefficient	$1.000 \times 10^1$
33	$k_{15}$	CRY2n degradation rate	$1.000 \times 10^1$
34	$Km_8$	CRY2n degradation inhibition	$1.829 \times 10^{-2}$

ponents would help in conferring confidence to model predictions.

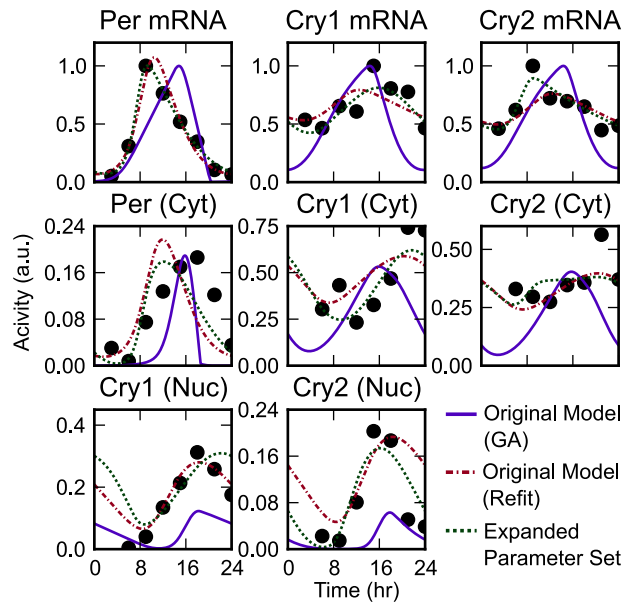
Two sensitivities, the PER translation rate (figure 3.5B, 1) and the PER-CRY association rate (2), had high confidence and consistent direction in both the base and expanded parameterization - suggesting that the predicted values are robust to slight changes in both parameter value and model structure. Since a biological system can be modeled using many different combinations of kinetic assumptions, such a technique will likely prove useful in finding consistent predictions which are robust to slight differences in model equations.

Figure 3.6 compares optimal fits for both the base and expanded models to the originally published parameter set [3]. Since the original cost function was concerned mostly with optimizing stoichiometric and knockout data, the refitted models are able to much more accurately represent the time-series dynamics.

## 3.4 Conclusions

Increasingly, mathematical models are being used to study biological systems where traditional experiments would prove infeasible. For example, in the search for drug targets, thousands of possible combinatorial perturbations can be quickly scanned for therapeutic effects using *in silico* modeling. This is especially useful in oscillatory systems with long periods, such as circadian rhythms, where a perturbed *in vitro* or *in vivo* system must be measured for multiple days before changes can be reliably determined.

However, since errors in model responses can arise from either incorrect structure or measurement noise, our confidence in *in silico* predictions is limited. Here we have developed a bootstrap approach suitable for periodic systems, and extended it to include uncertainty in predicted responses. With this method, errors due to local parameter effects can be identified, even in models with complicated dynam-



**Figure 3.6: Time-Series Dynamics of Fitted Models.** Model trajectories for each of the considered models. The original model (purple) shows the time series dynamics for the previously published parameter set, used in Figures 1-4. In these plots, the original model's period and amplitudes were rescaled to best match the experimental data, shown in black (without changing the dynamic profiles). The refitted model (red, dashed) was generated by optimizing the dynamic profile to time series data using the parameter estimation routine described in Supplemental Text 1. The expanded model (green, dashed) consists of a similar network structure, but with independent kinetic parameters for each rate expression (see Supplemental Text 2). These plots show that parameter optimization through nonlinear programming is able to more accurately fit gene and protein expression profiles.

ics. Furthermore, by considering multiple variations in model assumptions, we have demonstrated that more trustworthy model predictions can be found.

Since this method takes advantage of time-series data to generate a strong initial guess for an otherwise difficult parameter estimation, it requires high-resolution data on the concentrations of all species in the model. In many biological systems, such data is only available for the activity levels of certain well-studied species. However, the continued development of high-throughput genomic and proteomic techniques promise to deliver time-series data for a much larger network of components. With expanding datasets, these methods will likely prove useful for the quantitative evaluation of uncertainty in larger biological models.

In the following chapter, I apply this method to several existing circadian models in order find conserved predictions across different model kinetics and parameterizations. Such an approach allows us to further differentiate between the actions of two seemingly similar small molecule perturbations.

# Chapter 4

## Spatiotemporal separation of PER and CRY posttranslational regulation<sup>1</sup>

In the previous chapter, computationally efficient techniques for performing a bootstrap analysis on circadian models was described. In this chapter, we apply this technique to clarify the roles of two posttranslational regulators in the core circadian feedback loop. Since direct experimental evidence of the systems-level effect of these regulators is difficult if not impossible to obtain, we must rely on computational modeling to provide insight into the dynamic consequences of modulating posttranslational activity. For this reason, bootstrap methods are invaluable in generating confident *in silico* results.

### 4.1 Background

Since circadian and metabolic regulators are tightly integrated, circadian disruptions often manifest in metabolic disease [45]. Recent efforts have therefore sought to gain a mechanistic understanding of these pathways, such that the metabolic burdens

---

<sup>1</sup>Portions of this chapter are published in P. C. St. John, T. Hirota, S. A. Kay, and F. J. Doyle, "Spatiotemporal separation of PER and CRY posttranslational regulation in the mammalian circadian clock," *Proc. Natl. Acad. Sci. U. S. A.*, vol. 111, pp. 2040–5, Feb. 2014.

imposed by a 24-hour society might be mitigated. Posttranslational regulators, which play key roles in connecting circadian and metabolic processes, serve as likely targets for future therapeutics – demonstrated by the wealth of available circadian-active small molecules [2].

#### 4.1.1 Nuclear entry of PER-CRY complex

Oscillations in circadian gene transcription are generated through a time-delayed transcription-translation negative-feedback loop. In mammals, transcription factors CLOCK and BMAL1 promote transcription of E box-containing genes *Period* (*Per*) and *Cryptochrome* (*Cry*) (figure 4.1). PER and CRY protein products form heterodimers to accumulate in the nucleus, in which PER is stoichiometrically limiting [13], and subsequently close the negative feedback loop by inhibiting CLOCK-BMAL1-promoted gene expression. While steady-state endpoint assays have shown the possibility of nuclear entry of CRY without PER [9, 46, 47], experiments from *Per1*<sup>-/-</sup> *Per2*<sup>-/-</sup> mice demonstrated that PER proteins are required for the timely nuclear accumulation of CRY [13]. Clearance of nuclear repressors reactivates CLOCK-BMAL1, allowing the cycle to begin anew [48].

Experimental evidence on PER/CRY nuclear entry is seemingly contradictory. For nuclear localization of the PER and CRY proteins, experiments from *Per1*<sup>-/-</sup> *Per2*<sup>-/-</sup> mice demonstrate that PER proteins are required for timely nuclear accumulation of CRY [13]. While other studies have shown the possibility of nuclear entry of CRY without PER, these results are typically based on steady-state endpoint assays which do not consider the speed of CRY nuclear entry [9, 46, 47]. We therefore consider the formation of the PER-CRY heterodimer as a key step in nuclear entry, which is supported by the fact that to the best of our knowledge all circadian models that consider both PER and CRY employ this kinetic assumption [3, 10, 11, 12, 22].

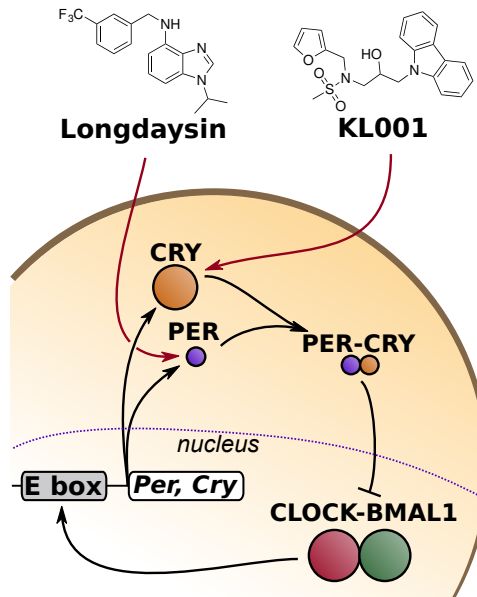


**Figure 4.1: Small molecule targets.** Schematic of the core circadian feedback loop, with the targets of small molecule modulators longdaysin (CKI inhibitor) and KL001 (inhibitor of FBXL3-dependent CRY degradation) shown. The size of each molecule is representative of relative concentration

#### 4.1.2 Importance of posttranslational regulators

The stabilities of PER and CRY are tightly regulated: PER proteins are phosphorylated by the casein kinase I family of proteins (CKI $\delta$ / $\epsilon$ ), prompting  $\beta$ -TrCP-mediated degradation [49] and nuclear import [50]. The degradation of CRY proteins is separately regulated by the SCF<sup>FBXL3</sup> ubiquitin ligase complex [51, 52, 53]. The activities of both CKI-PER and FBXL3-CRY may be further coupled to the cell's metabolic state through AMPK signalling [54]. These posttranslational regulatory mechanisms have a strong effect on period length: the gain-of-function mutant CKI $\epsilon$ <sup>tau</sup> leading to hyperphosphorylation of PER [55] and small molecule CKI inhibitors, such as longdaysin [32], demonstrated that increasing or decreasing CKI-dependent PER phosphorylation shortens or lengthens the period, respectively. In contrast, genetic mutations of FBXL3 [52, 53] and KL001, a small molecule inhibitor of FBXL3-dependent CRY degradation [3], showed that increased CRY stability leads to longer periods.

Since the scale and complexity of the circadian network complicates an intuitive understanding of these relationships, mathematical models have played important roles in understanding how these manipulations affect circadian period [3, 49, 55].

#### 4.1.3 Functional differences between PER and CRY

Given that both CKI and FBXL3 pathways regulate the stability of linked negative factors, it was thought that simultaneous perturbations to both pathways might lead to non-additive effects: i.e., the slowest link would determine the period. However, both small molecule [3] and genetic experiments [56] have demonstrated the independent period effects of these two posttranslational regulations. A recent clarification of the canonical clock feedback circuit has shown that dissociated CRY is the dominant repressor of CLOCK-BMAL1 mediated E box transcription [46]. This distinction helps differentiate between the roles of the otherwise similar PER and CRY proteins, in which the main role of PER in transcriptional repression is likely regulating the timing of nuclear accumulation of CRY. Therefore, while previous mathematical models in which PER acts as a direct repressor have proposed mechanisms for CKI-dependent period lengthening [55, 57], they are likely not suitable for distinguishing between CKI-PER and FBXL3-CRY mediated period change.

In this chapter, we used human cells harboring clock gene reporters together with mathematical modeling to gain insight into the relationship between PER and CRY posttranslational regulation. Consequently, we provide a new mechanism by which CKI-dependent PER phosphorylation controls the circadian period separately from the FBXL3-CRY pathway. The resulting detailed understanding of PER and CRY regulation in the core feedback loop provides a framework on which to interpret metabolic and pharmacological control of circadian rhythms.

## 4.2 Materials and Methods

### 4.2.1 Analysis of luminescence profiles

Raw luminescence data was first separated into a moving baseline and oscillatory component using a Hodrick-Prescott filter with a smoothing parameter of 1600. Example trajectory decompositions are shown in figure 4.2. Amplitudes (as shown in Fig. 1C) were determined by taking the standard deviation in the baseline-subtracted data. Periods were obtained by nonlinear curve fitting, in which a four parameter (initial amplitude, decay, period and phase) damped cosine curve was fit to the baseline-subtracted data. Periods were not shown if the relative amplitude (found by standard deviation) fell below 25%, since noise dominated the periodic trajectory.

### 4.2.2 Cost function

Models were fit to a cost function of experimental results. *Per*, *Cry*, *Clock*, and *Bmal1* protein and mRNA levels were taken from [13], along with profiles of CRY nuclear localization. For the model from [22], additional activity profiles on *Rev-Erb* and *Ror* were obtained from CircaDB (<http://bioinf.itmat.upenn.edu/circa/>). To score a model trajectory, mRNA state variables were scaled independently to minimize the squared error between model and experiment, since model parameters could be adjusted to give mRNA profiles arbitrary amplitudes. For protein species, where stoichiometric interactions are important, a single scaling parameter was used for all species. Nuclear repressor species, in which only relative measurements were available, were scaled independently. Full model equations for the model from Hirota *et al.*, 2012 are shown in table 2.1, the model from Relógio *et al.* 2011 in table 4.1, and the model from Leloup & Goldbeter, 2003 in table 4.2.

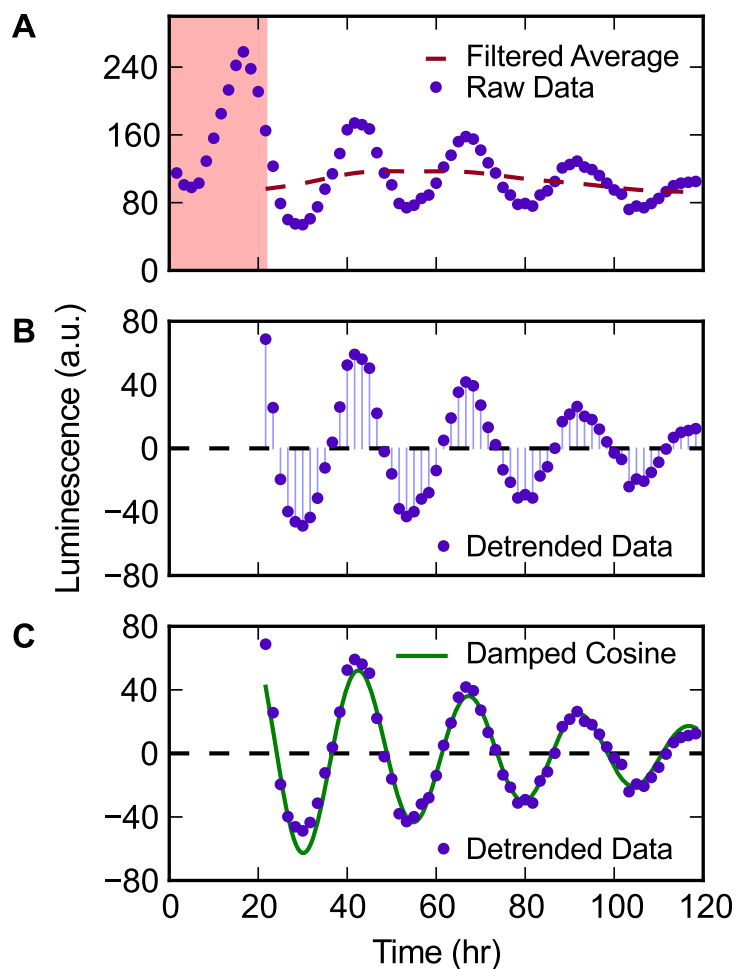


**Figure 4.2: Analysis of circadian reporter luminescence data.** (A) Raw luminescence data is first cropped by removing the initial transient region (first 12 points). The moving baseline is estimated using a Hodrick-Prescott filter with smoothing parameter 1600 (red dashed line). (B) Data is detrended by subtracting the moving baseline from the raw data. The detrended data is used to calculate the relative amplitude of the oscillations via standard deviation. (C) Periods are estimated by fitting a damped cosine curve (green solid line) to the detrended data.

**Table 4.1: Model equations for the model from Relógio *et al.* 2011 [22].**

$$\begin{aligned}
 \frac{d \text{CLKBM1}}{dt} &= \text{BM1n} \cdot k_f \text{CLKBM1} - \text{CLKBM1} \cdot d\text{CLKBM1} - \text{CLKBM1} \cdot k_d \text{CLKBM1} \\
 \frac{d \text{reverb}}{dt} &= \frac{V3 \max \left( g \cdot \frac{\text{CLKBM1}^v}{k t^3} + 1 \right)}{\frac{\text{CLKBM1}^v}{k t^3} \left( \frac{PnCn + PnpCn}{k i^3} \right)^w + \frac{\text{CLKBM1}^v}{k t^3} + 1} - d\text{reverb} \cdot \text{reverb} \\
 \frac{d \text{ror}}{dt} &= \frac{V4 \max \left( h \cdot \frac{\text{CLKBM1}^p}{k t^4} + 1 \right)}{\frac{\text{CLKBM1}^p}{k t^4} \cdot \left( \frac{PnCn + PnpCn}{k i^4} \right)^q + \frac{\text{CLKBM1}^p}{k t^4} + 1} - d\text{ror} \cdot \text{ror} \\
 \frac{d \text{REVERBc}}{dt} &= -\text{REVERBc} \cdot d\text{REVERBc} - \text{REVERBc} \cdot k_i \text{REVERBc} + k_p 3 \cdot \text{reverb} \\
 \frac{d \text{RORc}}{dt} &= -\text{RORc} \cdot d\text{RORc} - \text{RORc} \cdot k_i \text{RORc} + k_p 4 \cdot \text{ror} \\
 \frac{d \text{REVERBn}}{dt} &= \text{REVERBc} \cdot k_i \text{REVERBc} - \text{REVERBn} \cdot d\text{REVERBn} \\
 \frac{d \text{RORn}}{dt} &= \text{RORc} \cdot k_i \text{RORc} - \text{RORn} \cdot d\text{RORn} \\
 \frac{d \text{bm1}}{dt} &= \frac{V5 \max \left( i \cdot \frac{\text{RORn}^n}{k t^5} + 1 \right)}{\frac{\text{REVERBn}^m}{k i^5} + \frac{\text{RORn}^n}{k t^5} + 1} - \text{bm1} \cdot d\text{bm1} \\
 \frac{d \text{BM1c}}{dt} &= -\text{BM1c} \cdot d\text{BM1c} - \text{BM1c} \cdot k_i \text{BM1c} + \text{bm1} \cdot k_p 5 \\
 \frac{d \text{BM1n}}{dt} &= \text{BM1c} \cdot k_i \text{BM1c} - \text{BM1n} \cdot d\text{BM1n} - \text{BM1n} \cdot k_f \text{CLKBM1} + \text{CLKBM1} \cdot k_d \text{CLKBM1} \\
 \frac{d \text{per}}{dt} &= \frac{V1 \max \left( a \cdot \frac{\text{CLKBM1}^b}{k t^1} + 1 \right)}{\frac{\text{CLKBM1}^b}{k t^1} \cdot \left( \frac{PnCn + PnpCn}{k i^1} \right)^c + \frac{\text{CLKBM1}^b}{k t^1} + 1} - d\text{per} \cdot \text{per} \\
 \frac{d \text{cry}}{dt} &= \frac{V2 \max \left( \frac{\text{CLKBM1}^{3 \cdot d}}{k t^2} + 1 \right)}{\left( \frac{\text{REVERBn}^{f1}}{k i^2} + 1 \right) \left( \frac{\text{CLKBM1}^3}{k t^2} + \frac{\text{CLKBM1}^e}{k t^2} \left( \frac{PnCn + PnpCn}{k i^2} \right)^f + 1 \right)} - \text{cry} \cdot d\text{cry} \\
 \frac{d \text{Cc}}{dt} &= -\text{Cc} \cdot \text{Pc} \cdot k_f \text{PcCc} - \text{Cc} \cdot \text{Pcp} \cdot k_f \text{PcpCc} - \text{Cc} \cdot d\text{Cc} + \text{PcCc} \cdot k_d \text{PcCc} + \text{PcpCc} \cdot k_d \text{PcpCc} + \text{cry} \cdot k_p 2 \\
 \frac{d \text{Pc}}{dt} &= -\text{Cc} \cdot \text{Pc} \cdot k_f \text{PcCc} - \text{Pc} \cdot d\text{Pc} - \text{Pc} \cdot k_p h \text{Pc} + \text{PcCc} \cdot k_d \text{PcCc} + \text{Pcp} \cdot k_d \text{pH} \text{Pcp} + k_p 1 \cdot \text{per} \\
 \frac{d \text{Pcp}}{dt} &= -\text{Cc} \cdot \text{Pcp} \cdot k_f \text{PcpCc} + \text{Pc} \cdot k_p h \text{Pc} - \text{Pcp} \cdot d\text{Pcp} - \text{Pcp} \cdot k_d \text{pH} \text{Pcp} + \text{PcpCc} \cdot k_d \text{PcpCc} \\
 \frac{d \text{PcpCc}}{dt} &= \text{Cc} \cdot \text{Pcp} \cdot k_f \text{PcpCc} - \text{PcpCc} \cdot d\text{PcpCc} - \text{PcpCc} \cdot k_d \text{PcpCc} - \text{PcpCc} \cdot k_i \text{PcpCc} + \text{PnpCn} \cdot k_e \text{PnpCn} \\
 \frac{d \text{PcCc}}{dt} &= \text{Cc} \cdot \text{Pc} \cdot k_f \text{PcCc} - \text{PcCc} \cdot d\text{PcCc} - \text{PcCc} \cdot k_d \text{PcCc} - \text{PcCc} \cdot k_i \text{PcCc} + \text{PnCn} \cdot k_e \text{PnCn} \\
 \frac{d \text{PnpCn}}{dt} &= \text{PcpCc} \cdot k_i \text{PcpCc} - \text{PnpCn} \cdot d\text{PnpCn} - \text{PnpCn} \cdot k_e \text{PnpCn} \\
 \frac{d \text{PnCn}}{dt} &= \text{PcCc} \cdot k_i \text{PcCc} - \text{PnCn} \cdot d\text{PnCn} - \text{PnCn} \cdot k_e \text{PnCn}
 \end{aligned}$$

**Table 4.2: Model equations for the model from Leloup & Goldbeter, 2003 [10].**

$$\begin{aligned}
 \frac{dMP}{dt} &= -MP \cdot kdmp - \frac{MP \cdot vmP}{KmP + MP} + \frac{vsP \cdot BN^n}{BN^n + KAP^n} \\
 \frac{dMC}{dt} &= -MC \cdot kdmc - \frac{MC \cdot vmC}{KmC + MC} + \frac{vsC \cdot BN^n}{BN^n + KAC^n} \\
 \frac{dMB}{dt} &= -MB \cdot kdmb - \frac{MB \cdot vmB}{KmB + MB} + \frac{vsB \cdot KIB^m}{BN^m + KIB^m} \\
 \frac{dPC}{dt} &= -CC \cdot PC \cdot k3 + MP \cdot ksP - \frac{PC \cdot V1P}{Kp + PC} - PC \cdot kdn + PCC \cdot k4 + \frac{PCP \cdot V2P}{Kdp + PCP} \\
 \frac{dCC}{dt} &= -CC \cdot PC \cdot k3 - \frac{CC \cdot V1C}{CC + Kp} - CC \cdot kdn + \frac{CCP \cdot V2C}{CCP + Kdp} + MC \cdot ksC + PCC \cdot k4 \\
 \frac{dPCP}{dt} &= \frac{PC \cdot V1P}{Kp + PC} - \frac{PCP \cdot V2P}{Kdp + PCP} - PCP \cdot kdn - \frac{PCP \cdot vdPC}{Kdp + PCP} \\
 \frac{dCCP}{dt} &= \frac{CC \cdot V1C}{CC + Kp} - \frac{CCP \cdot V2C}{CCP + Kdp} - CCP \cdot kdn - \frac{CCP \cdot vdCC}{CCP + Kd} \\
 \frac{dPCC}{dt} &= CC \cdot PC \cdot k3 - \frac{PCC \cdot V1PC}{Kp + PCC} - PCC \cdot k1 - PCC \cdot k4 - PCC \cdot kdn + \frac{PCCP \cdot V2PC}{Kdp + PCCP} + PCN \cdot k2 \\
 \frac{dPCN}{dt} &= -BN \cdot PCN \cdot k7 + IN \cdot k8 + PCC \cdot k1 - \frac{PCN \cdot V3PC}{Kp + PCN} - PCN \cdot k2 - PCN \cdot kdn + \frac{PCNP \cdot V4PC}{Kdp + PCNP} \\
 \frac{dPCCP}{dt} &= \frac{PCC \cdot V1PC}{Kp + PCC} - \frac{PCCP \cdot V2PC}{Kdp + PCCP} - PCCP \cdot kdn - \frac{PCCP \cdot vdPCC}{Kd + PCCP} \\
 \frac{dPCNP}{dt} &= \frac{PCN \cdot V3PC}{Kp + PCN} - \frac{PCNP \cdot V4PC}{Kdp + PCNP} - PCNP \cdot kdn - \frac{PCNP \cdot vdPCN}{Kd + PCNP} \\
 \frac{dBC}{dt} &= \frac{-BC \cdot V1B}{BC + Kp} - BC \cdot k5 - BC \cdot kdn + \frac{BCP \cdot V2B}{BCP + Kdp} + BN \cdot k6 + MB \cdot ksB \\
 \frac{dBCP}{dt} &= \frac{BC \cdot V1B}{BC + Kp} - \frac{BCP \cdot V2B}{BCP + Kdp} - BCP \cdot kdn - \frac{BCP \cdot vdBC}{BCP + Kd} \\
 \frac{dBN}{dt} &= BC \cdot k5 - BN \cdot PCN \cdot k7 - \frac{BN \cdot V3B}{BN + Kp} - BN \cdot k6 - BN \cdot kdn + \frac{BNP \cdot V4B}{BNP + Kdp} + IN \cdot k8 \\
 \frac{dBNP}{dt} &= \frac{BN \cdot V3B}{BN + Kp} - \frac{BNP \cdot V4B}{BNP + Kdp} - BNP \cdot kdn - \frac{BNP \cdot vdBN}{BNP + Kd} \\
 \frac{dIN}{dt} &= BN \cdot PCN \cdot k7 - IN \cdot k8 - IN \cdot kdn - \frac{IN \cdot vdIN}{IN + Kd}
 \end{aligned}$$

### 4.2.3 Parameter estimation and bootstrap analysis

Bootstrap parameter estimations were performed as described previously [58], with data from [13] assumed to have a normally distributed 10% relative and 5% absolute error. Since not all states in the models were measured, initial guess values for the trajectory and parameter variables were generated by optimizing the parameter sets first with a genetic algorithm approach, described in [11]. To help ensure bootstrap trials remained in a similar stability region of parameter space (and protect against steady-state solutions), bootstrap parameters were bound between 50% and 150% of their initial value.

### 4.2.4 Selection of parameters for FBXL3-CRY and CKI-PER mechanisms

For FBXL3-CRY, parameters that determined the degradation rate of CRY (or CRY containing complexes) were considered to be the most likely candidates. Michealis-Menten degradation parameters were omitted from Fig. 3 since perturbations to such parameters are not easily attributable to changes in FBXL3 binding affinity. In the model presented in [10], CRY is degraded through a series of phosphorylation events, and these parameters were considered as representative of the rate of progression toward ubiquitination of CRY. The forward phosphorylation rates of CRY and nuclear PER-CRY complex were therefore also considered. For CKI-PER, we considered rates that determined the degradation rate and nuclear import rate of PER. Michealis-Menten parameters were not included, similar to FBXL3-CRY. With CRY being the main repressor of E box transcription [46], the degradation rates of PER-CRY complex were not considered as potential mechanisms of CKI. In the models of [10] and [22], the nuclear entry of PER-CRY requires two independent steps: the formation of the PER-CRY complex and the subsequent import of the complex. Therefore, the forward

reaction rates of each of these steps were included.

### 4.2.5 Numerical experiments

Numerical parameter inhibitions were performed by recalculating the limit cycle trajectory for each new parameter set to a tolerance of  $10^{-8}$ , using computational methods described previously [21].

## 4.3 Results and Discussion

### 4.3.1 Opposite amplitude effects of longdaysin and KL001

To gain a more detailed understanding of the roles of CKI-PER and FBXL3-CRY pathways, we applied small molecule compounds longdaysin and KL001, which cause stabilization of PER and CRY, respectively [3, 32] (figure 4.1). We used *Bmal1*- and *Per2-dLuc* as circadian reporters, which represent different loops of the core clock mechanism and show circadian luminescence rhythms with mutually opposite phase. Time-course data on circadian reporter expression under increasing concentrations of longdaysin and KL001 [3] was analyzed for period and amplitude change (figure 4.3). Longdaysin caused dose-dependent increases in period and detrended amplitude to  $\approx 50\%$  of control values in both *Bmal1*- and *Per2-dLuc* reporter cells. In contrast, KL001 induced a simultaneous increase in period and strong reduction in amplitude. Modulation of the activity of CKI-PER and FBXL3-CRY is therefore differentiated by an opposite amplitude response.

### 4.3.2 Main period-determining perturbations

We next used *in silico* modeling to gain mechanistic insight into CKI-PER and FBXL3-CRY mediated circadian regulation. In chapter 2, I described the connection between

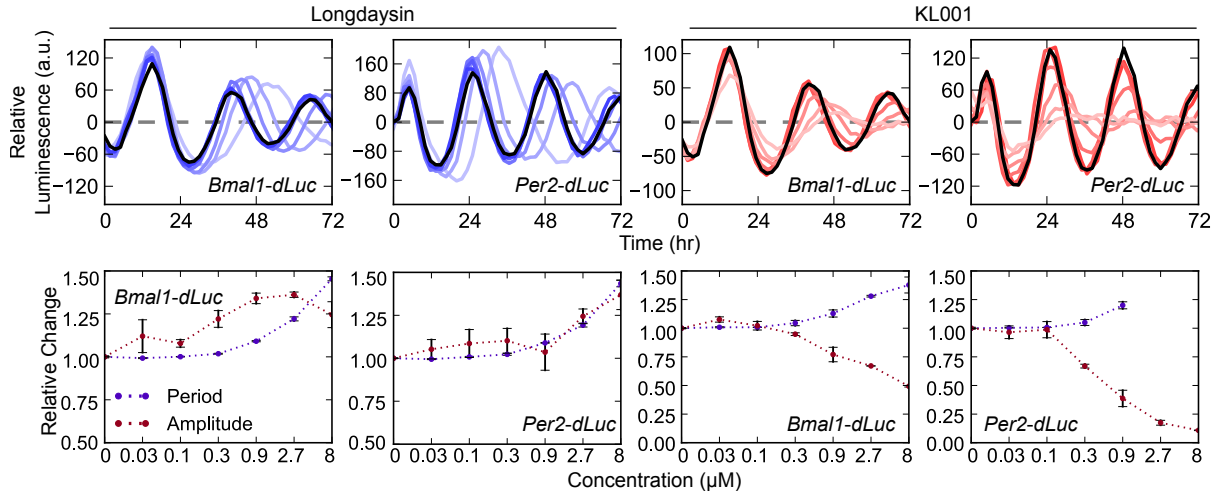


**Figure 4.3: Different amplitude effect of small molecule circadian modulators targeting CKI-PER and FBXL3-CRY.** (top) Detrended luminescence profiles (first 72 hours, mean of two independent replications) obtained from U2OS reporter cells with increasing concentration of longdaysin and KL001. Black profiles indicate control conditions ( $0 \mu\text{M}$ ), lighter colors indicate higher concentrations of small molecule (from  $0.03$  to  $8 \mu\text{M}$ ). (bottom) Relative change in period and amplitude of the results in shown on top.

inhibition of FBXL3-dependent CRY degradation and period change [3]: increasing the stability of nuclear CRY results in longer transcriptional repression and increased period length. However, while CKI has been linked to modulating PER stability and nuclear entry, it remained unclear which perturbation dominates the period effect, and whether these processes are sufficient to separate the effects of CKI and FBXL3.

To generate predictions that are consistent across slight differences in model assumptions, we chose three mathematical models from the literature based on their moderate size and similar scope [3, 10, 22]. The models included, at a minimum, the expression and nuclear entry mechanisms of PER and CRY. We considered the formation of the PER-CRY heterodimer as a key step in nuclear entry, which is supported by the fact that, to the best of our knowledge, all circadian models that consider both PER and CRY employ this kinetic assumption [3, 10, 11, 12, 22].

Since dynamic models of genetic regulatory networks typically suffer from poor

parameter identifiability [59], we demonstrate that our predictions are parameter-independent by employing a bootstrap identifiability analysis [58]. As part of the bootstrap method, the models were re-fit to experimental data [13] while ensuring appropriate protein stoichiometry. The state trajectories of the resulting 2000 parameter sets for each model are shown in figure 4.4, with reasonable agreement between models and experiment.

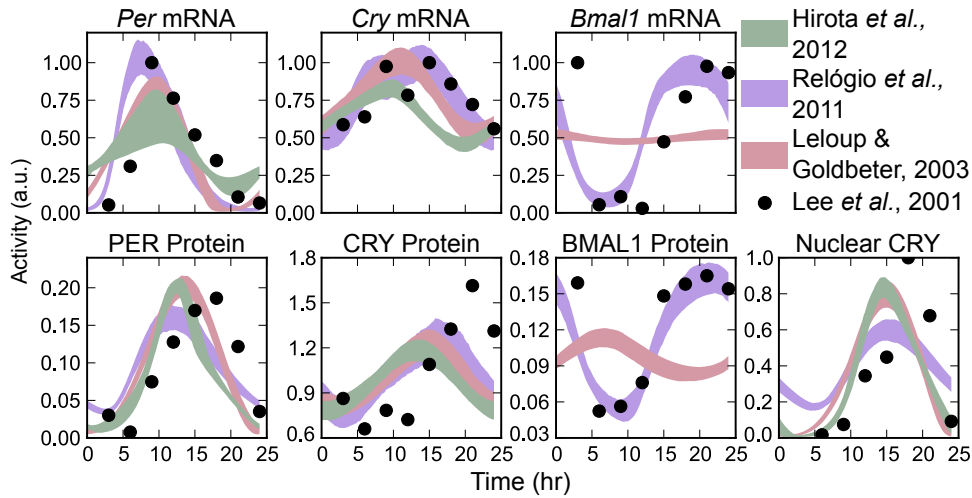


**Figure 4.4: Fitted trajectories from bootstrap runs.** Time series trajectories of the 2000 bootstrap trials for each model. Shaded regions indicate 95% confidence regions. The data were scaled to have a maximum value of 1, except for protein species, where relative values were important for clock stoichiometry.

A first-order period sensitivity analysis, performed on each of the parameter sets, identified which parameters associated with PER and CRY protein activity had the greatest effect on period (figure 4.5). To simplify analysis, we present only those parameters that are associated with experimentally supported mechanisms of CKI and FBXL3 in figure 4.6. We first tested parameters associated with potential FBXL3-CRY activity to evaluate if our method matched the experimentally verified effect of KL001 [3]. Since CRY is the dominant repressor of CLOCK-BMAL1 [46], we attribute degradation rates of the PER-CRY complex to be representative of CRY clearance rates. We found that only parameters governing nuclear CRY degradation show

a period lengthening effect upon inhibition, while rates associated with cytoplasmic CRY degradation show period shortening effects. These results match with our previous assertion that period lengthening occurs via nuclear CRY stabilization [3]. Experimental evidence has also indicated cytoplasmic CRY stabilization may lead to period shortening [16], a result consistent with our mathematical results.

We next describe parameters potentially associated with CKI-dependent regulation of PER localization and stability. Since PER is rate-limiting in the formation of the PER-CRY complex [13], rates associated with complex formation or nuclear import were included in this analysis. Conversely, we did not include degradation rates of PER-CRY nuclear repressive complex, since CRY alone is considered the main repressor. While it was hypothesized in models where PER acts as a direct repressor that the regulation of PER stability would play the dominant role determining the period [55, 57], our new assumptions revealed that parameters governing PER degradation showed only non-identifiable responses. However, inhibition of rates associated with the nuclear entry of the PER-CRY complex showed strong period lengthening effects. These results indicate that under our current understanding of clock kinetics, the regulation of nuclear import likely plays the prominent role in CKI-dependent period regulation.

### 4.3.3 Independent mechanisms of PER and CRY regulation

Using the model and parameter set of Hirota *et al.*, 2012 [3] and the perturbations identified in figure 4.6, we first confirmed that inhibition of nuclear CRY degradation (vdCn) and PER-CRY nuclear import (vaC1P) reproduced the experimental period and amplitude effects of the small molecules KL001 and longdaysin, respectively (figure 4.7, compare with figure 4.3).

Comparison of the oscillatory profiles of *Per* mRNA and nuclear CRY protein (Fig. 4B) revealed that inhibition of FBXL3-dependent CRY degradation caused lingering

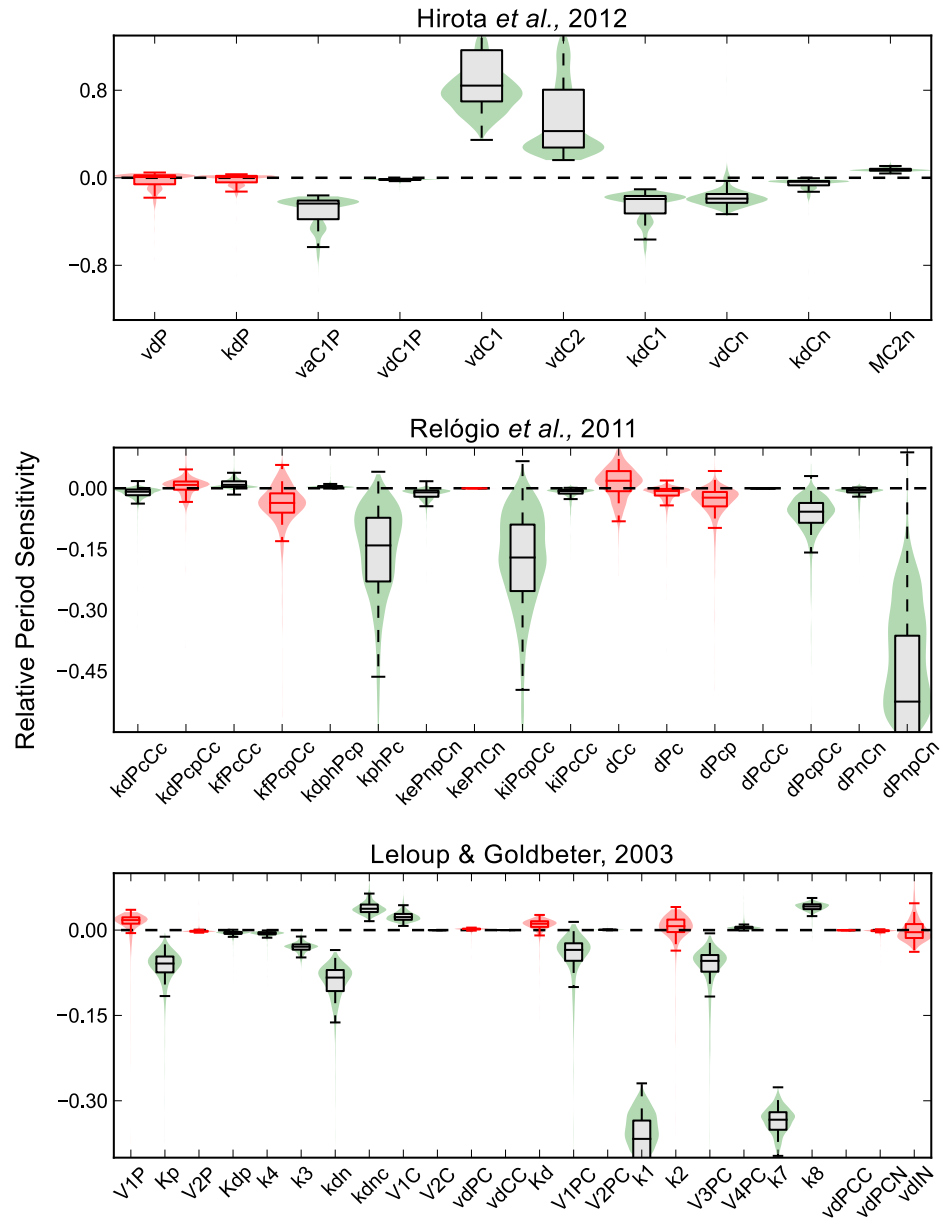


**Figure 4.5: Bootstrap confidence intervals in relative period sensitivities.**  
 Violin plots for distributions in relative period sensitivities for parameters associated with PER and CRY proteins. Whiskers extend to the most extreme data point within  $1.5 \times$  the inner quartile range. Distributions in which the 5<sup>th</sup> and 95<sup>th</sup> percentile lie on opposite sides of the x-axis are colored red and deemed non-identifiable.

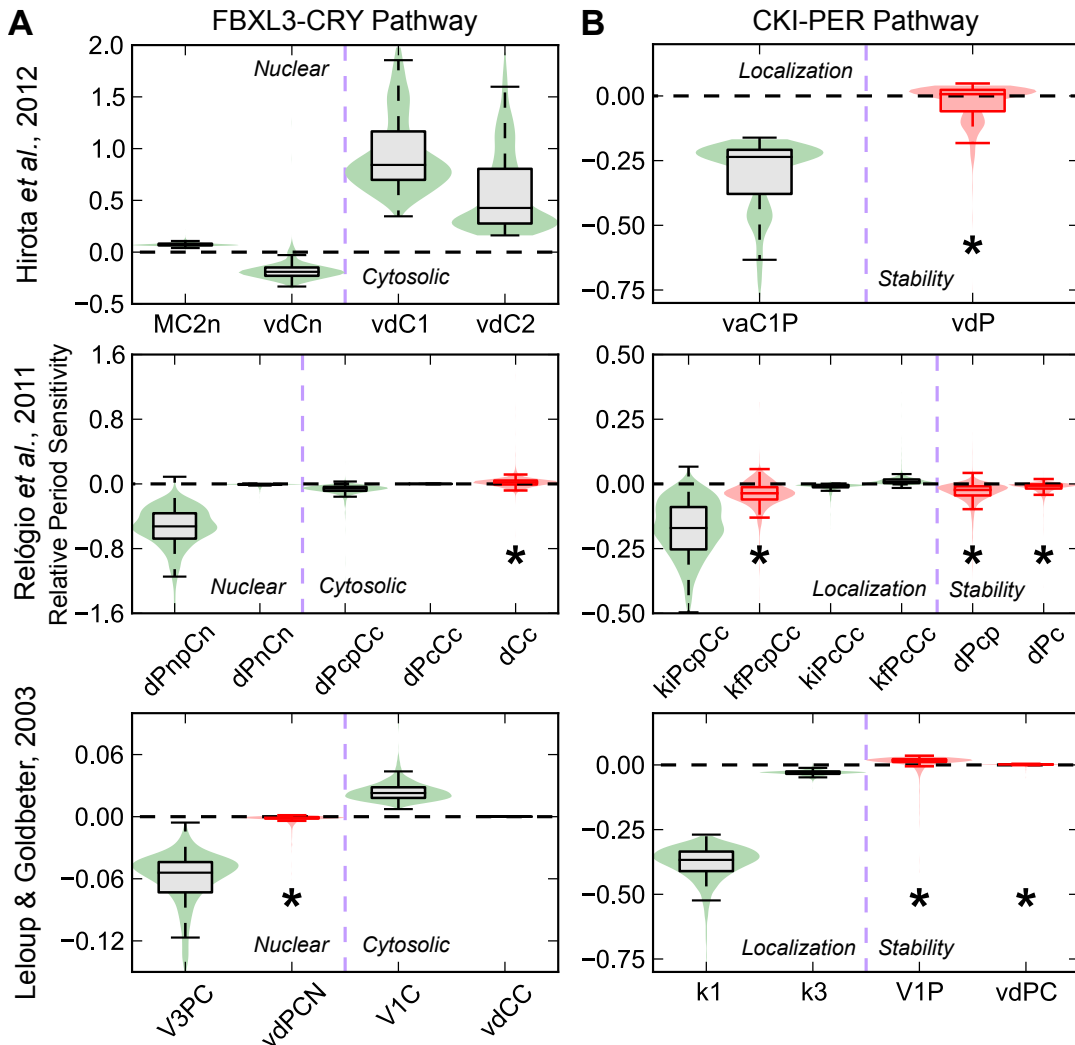


**Figure 4.6: Bootstrap predictions of circadian actions of FBXL3-CRY and CKI-PER pathways.** Violin plots of the relative period sensitivity of parameters associated with potential mechanisms for FBXL3-CRY (A) and CKI-PER (B) activity. A negative or positive period sensitivity indicate that the period of oscillation will increase or decrease when that rate is inhibited, respectively. Distributions that are not different than 0 with 95% confidence are colored red. Descriptions of the parameters shown are listed in tables 4.3-4.4.

**Table 4.3:** Descriptions of the model parameters governing FBXL3-CRY

Model	Parameter	Description
[3]	MC2n	CRY2 nuclear multiplicative degradation coefficient
	vdCn	CRY1/2 nuclear degradation rate
	vdC1	CRY1 cytoplasmic degradation rate
	vdC2	CRY2 cytoplasmic degradation rate
[22]	dPnpCn	Phosphorylated PER-CRY complex nuclear degradation rate
	dPnCn	PER-CRY complex nuclear degradation rate
	dPcpCc	Phosphorylated PER-CRY complex cytoplasmic degradation rate
	dPcCc	PER-CRY complex cytoplasmic degradation rate
	dCc	CRY cytoplasmic degradation rate
[10]	V3PC	PER-CRY complex nuclear phosphorylation rate
	vdPCN	Phosphorylated PER-CRY complex nuclear degradation rate
	V1C	CRY cytoplasmic degradation rate
	vdCC	Phosphorylated CRY cytoplasmic degradation rate

**Table 4.4:** Descriptions of the model parameters governing CKI-PER

Model	Parameter	Description
[3]	vaC1P	PER-CRY complex nuclear entry rate
	vdP	PER cytoplasmic degradation rate
[22]	kiPcpCc	Phosphorylated PER-CRY complex nuclear entry rate
	kfPcpCc	Phosphorylated PER-CRY complex association rate
	kiPcCc	PER-CRY complex nuclear entry rate
	kfPcCc	PER-CRY complex association rate
	dPcp	Phosphorylated PER cytoplasmic degradation rate
	dPc	PER cytoplasmic degradation rate
[10]	k1	PER-CRY complex nuclear entry rate
	k3	PER-CRY complex association rate
	V1P	PER cytoplasmic phosphorylation rate
	vdPC	Phosphorylated PER cytoplasmic degradation rate

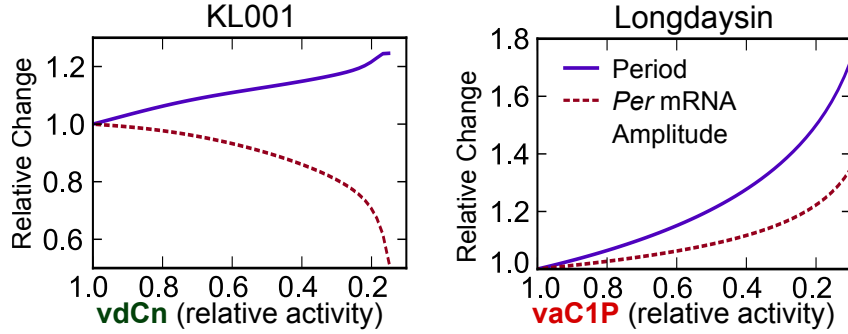


**Figure 4.7: Predictions of KL001 and longdaysin results.** *In silico* reproductions of the circadian reporter experiments in figure 4.3, using the predictions identified in figure 4.6.

nuclear CRY to not be completely purged each cycle. This excess repressor during the accumulating phase of *Per* and *Cry* transcripts resulted in lower E box amplitudes, providing a likely explanation for the effect of KL001.

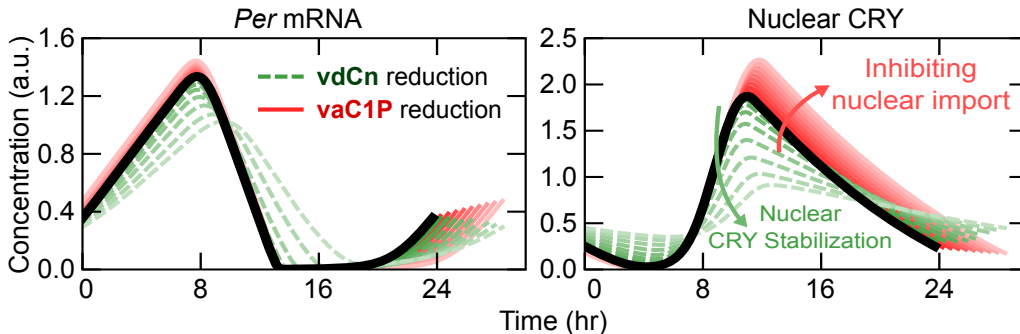


**Figure 4.8: Comparison of the effects of KL001 and longdaysin.** Parameter changes were normalized such that the period change was equal for each pair of perturbations (vdCn: 100%  $\rightarrow$  23%, vaC1P: 100%  $\rightarrow$  51%).

In contrast, stabilization of cytoplasmic PER (lowering vdp) resulted in reduced transcriptional amplitude with minimal period effect (figure 4.9), consistent with experimental findings from the knockdown of  $\beta$ -TrCP, an F box protein responsible for PER degradation [60]. However, other experimental results have shown that down-regulation of  $\beta$ -TrCP leads to longer periods [49], suggesting that further modeling and experimental inquiry is needed on the role of  $\beta$ -TrCP in clock regulation. This period lengthening might be explained through  $\beta$ -TrCP-mediated stabilization of nuclear PER-CRY or by using alternative kinetic assumptions for the rate of PER-CRY

binding.

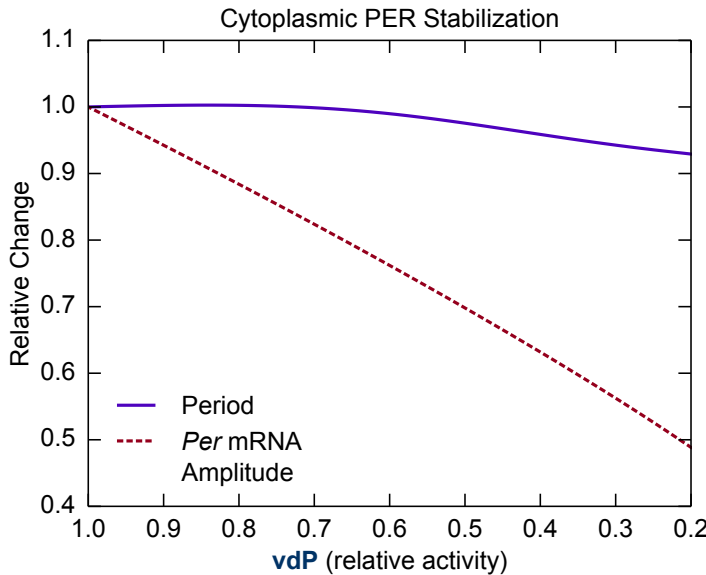


**Figure 4.9: Effect of cytoplasmic PER stabilization on period and E box transcription amplitude.** Relative period and peak-to-trough amplitude change in *Per* mRNA resulting from a reduction in the vdp parameter in the model from Hirota *et al.*, 2012.

We further compared the effect of inhibiting PER degradation with inhibiting nuclear import on the oscillatory profile of key clock proteins (figure 4.10) to identify mechanistic differences between the two potential effects of CKI inhibition. Both perturbations increased cytoplasmic PER, suggesting the two mechanisms are difficult to distinguish experimentally. Direct stabilization of PER in the cytoplasm (lowering vdp) lead to two simultaneous trends which shift the period in opposite directions: it shortened the time delay between transcription and inactivation by accelerating the accumulation of cytoplasmic PER and nuclear PER-CRY; and lengthened the repressive phase by increasing the total amount of PER-CRY which enters the nucleus. These perturbations sped and slowed the clock, respectively, and resulted in little period change. In contrast, inhibiting PER-CRY nuclear entry (lowering vaC1P) caused additional free protein to build in the cytoplasm, delaying nuclear accumulation and ultimately increasing the total amount of nuclear PER-CRY. Since both of these trends work to increase period length, inhibiting PER-CRY nuclear entry resulted in signif-

icantly longer cycles. Additionally, the longer cytoplasmic time delay resulted in increased transcription, yielding slightly higher amplitudes (figure 4.8) that closely match the experimental results of the small molecule longdaysin.

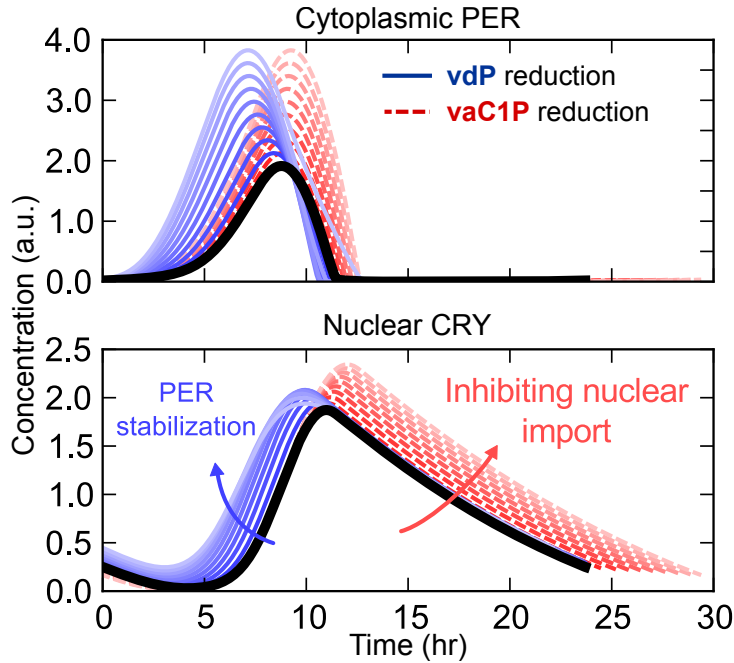


**Figure 4.10: Comparison of two candidate mechanisms for CKI inhibition.** Effects of increasing PER stabilization and nuclear import inhibition on the time profiles of cytoplasmic PER (top) and nuclear CRY (bottom). Parameter values were selected such that the amplitudes of cytoplasmic PER are equal at each level. Lighter colors indicate stronger perturbations (vdp: 100%  $\rightarrow$  22%, vac1P: 100%  $\rightarrow$  45%),  $t = 0$  is set to the onset of PER accumulation.

Since CKI likely regulates both stability and subcellular localization of PER *in vivo*, we considered the effects of simultaneously lowering both PER cytoplasmic degradation and nuclear entry rates (Fig. 5A). The loss of oscillations under extreme reduction of both parameters (Fig. 5A, shaded regions) highlights an interesting role of CKI in conferring robustness to the circadian clock: since oscillations are lost when import of the PER-CRY complex to the nucleus ceases to be rhythmic, CKI ensures lingering PER is purged from the cytoplasm by one pathway or another before E box transcription resumes. This importance has been proven experimentally,

as disruption of CKI-mediated regulation leads to compromised circadian oscillations [61].

Together, inhibition of CKI by longdaysin may increase the time required before PER-CRY can enter the nucleus to repress transcription, leading to a higher amplitude and longer period. In contrast, KL001 lengthens the period by stabilizing nuclear CRY, resulting in a longer time delay before transcription resumes and lower amplitude from increased E box repression. PER regulation through CKI is therefore partitioned to the accumulating phase, controlling the speed and amount of PER-CRY complex that enters the nucleus. CRY regulation through FBXL3 is partitioned independently to the repressive phase, controlling the length of time until CLOCK-BMAL1-dependent transcription resumes (Fig. 6). This independence was reproduced *in silico* by the simultaneous reduction of nuclear CRY degradation and PER-CRY nuclear import (Fig. 5B), where nonlinear interactions in amplitude and period between the two perturbations are all but absent.

#### 4.3.4 Conclusion

An understanding of the interactions between posttranslational regulators is crucial for the further development of circadian pharmacological reagents, as efficient modulation of clock function will assuredly come from simultaneous perturbations to many connected species. In this study, we used circadian reporter cells together with mathematical modeling to provide mechanistic insight into the differences of CKI- and FBXL3- mediated posttranslational regulation of PER and CRY. As a result, we clarified a process by which CKI exerts control over the circadian period, demonstrated through both the hyperphosphorylating CKI $\epsilon^{\text{tau}}$  mutant and small molecule CKI inhibitors, such as longdaysin. In developing our predictions, we have used multiple models and parameterizations to ensure our mechanisms are consistent across many *in silico* realizations. These results reinforce the notion that computational

modeling is essential in interpreting results in systems with complicated oscillatory feedback. Additionally, *in silico* analyses reveal hidden design principles of biological networks, as this work highlights the importance of the CKI family of kinases in conferring robustness to the circadian cycle.

# Chapter 5

## Amplitude metrics for cellular bioluminescence reporters

### 5.1 Motivation, link to previous chapter

Hello, here is some text without a meaning. This text should show what a printed text will look like at this place. If you read this text, you will get no information. Really? Is there no information? Is there a difference between this text and some nonsense like “Huardest gefburn”? Kjift – not at all! A blind text like this gives you information about the selected font, how the letters are written and an impression of the look. This text should contain all letters of the alphabet and it should be written in of the original language. There is no need for special content, but the length of words should match the language.

#### 5.1.1 Different enzymes control circadian rhythms at different phases

Hello, here is some text without a meaning. This text should show what a printed text will look like at this place. If you read this text, you will get no information. Really? Is there no information? Is there a difference between this text and some

nonsense like “Huardest gefburn”? Kjift – not at all! A blind text like this gives you information about the selected font, how the letters are written and an impression of the look. This text should contain all letters of the alphabet and it should be written in of the original language. There is no need for special content, but the length of words should match the language.

### **5.1.2 Perturbations likely have a time-dependent effect on amplitude**

Hello, here is some text without a meaning. This text should show what a printed text will look like at this place. If you read this text, you will get no information. Really? Is there no information? Is there a difference between this text and some nonsense like “Huardest gefburn”? Kjift – not at all! A blind text like this gives you information about the selected font, how the letters are written and an impression of the look. This text should contain all letters of the alphabet and it should be written in of the original language. There is no need for special content, but the length of words should match the language.

### **5.1.3 Comparison of Ukai vs Pulivarthy 2007**

Hello, here is some text without a meaning. This text should show what a printed text will look like at this place. If you read this text, you will get no information. Really? Is there no information? Is there a difference between this text and some nonsense like “Huardest gefburn”? Kjift – not at all! A blind text like this gives you information about the selected font, how the letters are written and an impression of the look. This text should contain all letters of the alphabet and it should be written in of the original language. There is no need for special content, but the length of words should match the language.

## 5.2 Single cell amplitude metrics

Hello, here is some text without a meaning. This text should show what a printed text will look like at this place. If you read this text, you will get no information. Really? Is there no information? Is there a difference between this text and some nonsense like “Huardest gefburn”? Kjift – not at all! A blind text like this gives you information about the selected font, how the letters are written and an impression of the look. This text should contain all letters of the alphabet and it should be written in of the original language. There is no need for special content, but the length of words should match the language.

### 5.2.1 Definition of amplitude metric

Hello, here is some text without a meaning. This text should show what a printed text will look like at this place. If you read this text, you will get no information. Really? Is there no information? Is there a difference between this text and some nonsense like “Huardest gefburn”? Kjift – not at all! A blind text like this gives you information about the selected font, how the letters are written and an impression of the look. This text should contain all letters of the alphabet and it should be written in of the original language. There is no need for special content, but the length of words should match the language.

### 5.2.2 Finite difference ARC

Hello, here is some text without a meaning. This text should show what a printed text will look like at this place. If you read this text, you will get no information. Really? Is there no information? Is there a difference between this text and some nonsense like “Huardest gefburn”? Kjift – not at all! A blind text like this gives you information about the selected font, how the letters are written and an impression of

the look. This text should contain all letters of the alphabet and it should be written in of the original language. There is no need for special content, but the length of words should match the language.

### **5.2.3 Derivation of sensitivity-based method**

Hello, here is some text without a meaning. This text should show what a printed text will look like at this place. If you read this text, you will get no information. Really? Is there no information? Is there a difference between this text and some nonsense like “Huardest gefburn”? Kjift – not at all! A blind text like this gives you information about the selected font, how the letters are written and an impression of the look. This text should contain all letters of the alphabet and it should be written in of the original language. There is no need for special content, but the length of words should match the language.

## **5.3 Population-level models**

Hello, here is some text without a meaning. This text should show what a printed text will look like at this place. If you read this text, you will get no information. Really? Is there no information? Is there a difference between this text and some nonsense like “Huardest gefburn”? Kjift – not at all! A blind text like this gives you information about the selected font, how the letters are written and an impression of the look. This text should contain all letters of the alphabet and it should be written in of the original language. There is no need for special content, but the length of words should match the language.

### 5.3.1 Definitions and diffusion-convection equation

Hello, here is some text without a meaning. This text should show what a printed text will look like at this place. If you read this text, you will get no information. Really? Is there no information? Is there a difference between this text and some nonsense like “Huardest gefburn”? Kjift – not at all! A blind text like this gives you information about the selected font, how the letters are written and an impression of the look. This text should contain all letters of the alphabet and it should be written in of the original language. There is no need for special content, but the length of words should match the language.

### 5.3.2 Circular statistics

Hello, here is some text without a meaning. This text should show what a printed text will look like at this place. If you read this text, you will get no information. Really? Is there no information? Is there a difference between this text and some nonsense like “Huardest gefburn”? Kjift – not at all! A blind text like this gives you information about the selected font, how the letters are written and an impression of the look. This text should contain all letters of the alphabet and it should be written in of the original language. There is no need for special content, but the length of words should match the language.

### 5.3.3 Inverting $p(\theta, \hat{t})$

Hello, here is some text without a meaning. This text should show what a printed text will look like at this place. If you read this text, you will get no information. Really? Is there no information? Is there a difference between this text and some nonsense like “Huardest gefburn”? Kjift – not at all! A blind text like this gives you information about the selected font, how the letters are written and an impression of

the look. This text should contain all letters of the alphabet and it should be written in of the original language. There is no need for special content, but the length of words should match the language.

### **5.3.4 Calculating $\bar{x}(\hat{t})$ and $\hat{x}(\hat{t})$**

Hello, here is some text without a meaning. This text should show what a printed text will look like at this place. If you read this text, you will get no information. Really? Is there no information? Is there a difference between this text and some nonsense like “Huardest gefburn”? Kjift – not at all! A blind text like this gives you information about the selected font, how the letters are written and an impression of the look. This text should contain all letters of the alphabet and it should be written in of the original language. There is no need for special content, but the length of words should match the language.

# Chapter 6

## Decay rate as proxy for cellular noise

# Chapter 7

## Conclusions and future work

### 7.1 Continuation of collaboration with Andrew

Hello, here is some text without a meaning. This text should show what a printed text will look like at this place. If you read this text, you will get no information. Really? Is there no information? Is there a difference between this text and some nonsense like “Huardest gefburn”? Kjift – not at all! A blind text like this gives you information about the selected font, how the letters are written and an impression of the look. This text should contain all letters of the alphabet and it should be written in of the original language. There is no need for special content, but the length of words should match the language.

#### 7.1.1 Experimental validation of model predictions

Hello, here is some text without a meaning. This text should show what a printed text will look like at this place. If you read this text, you will get no information. Really? Is there no information? Is there a difference between this text and some nonsense like “Huardest gefburn”? Kjift – not at all! A blind text like this gives you information about the selected font, how the letters are written and an impression of

the look. This text should contain all letters of the alphabet and it should be written in of the original language. There is no need for special content, but the length of words should match the language.

### **7.1.2 Prediction of fasting perturbations**

Hello, here is some text without a meaning. This text should show what a printed text will look like at this place. If you read this text, you will get no information. Really? Is there no information? Is there a difference between this text and some nonsense like “Huardest gefburn”? Kjift – not at all! A blind text like this gives you information about the selected font, how the letters are written and an impression of the look. This text should contain all letters of the alphabet and it should be written in of the original language. There is no need for special content, but the length of words should match the language.

#### **small-molecule activators of SIRT1**

Hello, here is some text without a meaning. This text should show what a printed text will look like at this place. If you read this text, you will get no information. Really? Is there no information? Is there a difference between this text and some nonsense like “Huardest gefburn”? Kjift – not at all! A blind text like this gives you information about the selected font, how the letters are written and an impression of the look. This text should contain all letters of the alphabet and it should be written in of the original language. There is no need for special content, but the length of words should match the language.

### **7.1.3 Validity of step vs pulse perturbation**

Hello, here is some text without a meaning. This text should show what a printed text will look like at this place. If you read this text, you will get no information. Really? Is there no information? Is there a difference between this text and some nonsense like “Huardest gefburn”? Kjift – not at all! A blind text like this gives you information about the selected font, how the letters are written and an impression of the look. This text should contain all letters of the alphabet and it should be written in of the original language. There is no need for special content, but the length of words should match the language.

#### **Characterization of insulin effect**

Hello, here is some text without a meaning. This text should show what a printed text will look like at this place. If you read this text, you will get no information. Really? Is there no information? Is there a difference between this text and some nonsense like “Huardest gefburn”? Kjift – not at all! A blind text like this gives you information about the selected font, how the letters are written and an impression of the look. This text should contain all letters of the alphabet and it should be written in of the original language. There is no need for special content, but the length of words should match the language.

## **7.2 Amplitude maximization through therapeutic treatment**

Hello, here is some text without a meaning. This text should show what a printed text will look like at this place. If you read this text, you will get no information. Really? Is there no information? Is there a difference between this text and some

nonsense like “Huardest gefburn”? Kjift – not at all! A blind text like this gives you information about the selected font, how the letters are written and an impression of the look. This text should contain all letters of the alphabet and it should be written in of the original language. There is no need for special content, but the length of words should match the language.

### **7.2.1 Optimal control strategies to maximize peripheral clock amplitude**

Hello, here is some text without a meaning. This text should show what a printed text will look like at this place. If you read this text, you will get no information. Really? Is there no information? Is there a difference between this text and some nonsense like “Huardest gefburn”? Kjift – not at all! A blind text like this gives you information about the selected font, how the letters are written and an impression of the look. This text should contain all letters of the alphabet and it should be written in of the original language. There is no need for special content, but the length of words should match the language.

### **7.2.2 Fewest treatments, combinatorial perturbations, etc.**

Hello, here is some text without a meaning. This text should show what a printed text will look like at this place. If you read this text, you will get no information. Really? Is there no information? Is there a difference between this text and some nonsense like “Huardest gefburn”? Kjift – not at all! A blind text like this gives you information about the selected font, how the letters are written and an impression of the look. This text should contain all letters of the alphabet and it should be written in of the original language. There is no need for special content, but the length of words should match the language.

## 7.3 Iterative optimization of network topology

Hello, here is some text without a meaning. This text should show what a printed text will look like at this place. If you read this text, you will get no information. Really? Is there no information? Is there a difference between this text and some nonsense like “Huardest gefburn”? Kjift – not at all! A blind text like this gives you information about the selected font, how the letters are written and an impression of the look. This text should contain all letters of the alphabet and it should be written in of the original language. There is no need for special content, but the length of words should match the language.

### 7.3.1 (Idea from Mitsubishi proposal)

Hello, here is some text without a meaning. This text should show what a printed text will look like at this place. If you read this text, you will get no information. Really? Is there no information? Is there a difference between this text and some nonsense like “Huardest gefburn”? Kjift – not at all! A blind text like this gives you information about the selected font, how the letters are written and an impression of the look. This text should contain all letters of the alphabet and it should be written in of the original language. There is no need for special content, but the length of words should match the language.

### 7.3.2 Design machine-learning algorithm to find optimum model structure

Hello, here is some text without a meaning. This text should show what a printed text will look like at this place. If you read this text, you will get no information. Really? Is there no information? Is there a difference between this text and some nonsense like “Huardest gefburn”? Kjift – not at all! A blind text like this gives you

information about the selected font, how the letters are written and an impression of the look. This text should contain all letters of the alphabet and it should be written in of the original language. There is no need for special content, but the length of words should match the language.

# Bibliography

- [1] J. C. Dunlap, J. J. Loros, and P. J. DeCoursey, *Chronobiology: Biological Timekeeping*. Sinauer Associates, Inc., 2009.
- [2] Z. Chen, S.-H. Yoo, and J. S. Takahashi, "Small molecule modifiers of circadian clocks.," *Cell. Mol. Life Sci.*, vol. 70, pp. 2985–98, Aug. 2013.
- [3] T. Hirota, J. W. Lee, P. C. St. John, M. Sawa, K. Iwaisako, T. Noguchi, P. Y. Pongsawakul, T. Sonntag, D. K. Welsh, D. A. Brenner, F. J. Doyle, P. G. Schultz, and S. A. Kay, "Identification of Small Molecule Activators of Cryptochrome.," *Science*, vol. 337, pp. 1094–1097, July 2012.
- [4] E. V. McCarthy, J. E. Baggs, J. M. Geskes, J. B. Hogenesch, and C. B. Green, "Generation of a novel allelic series of cryptochrome mutants via mutagenesis reveals residues involved in protein-protein interaction and CRY2-specific repression," *Mol. Cell. Biol.*, vol. 29, pp. 5465–76, Oct. 2009.
- [5] G. T. van der Horst, M. Muijtjens, K. Kobayashi, R. Takano, S. Kanno, M. Takao, J. de Wit, A. Verkerk, A. P. Eker, D. van Leenen, R. Buijs, D. Bootsma, J. H. Hoeijmakers, and A. Yasui, "Mammalian Cry1 and Cry2 are essential for maintenance of circadian rhythms," *Nature*, vol. 398, pp. 627–30, Apr. 1999.
- [6] E. E. Zhang, A. C. Liu, T. Hirota, L. J. Miraglia, G. Welch, P. Y. Pongsawakul, X. Liu, A. Atwood, J. W. Huss, J. Janes, A. I. Su, J. B. Hogenesch, and S. A. Kay, "A genome-wide RNAi screen for modifiers of the circadian clock in human cells," *Cell*, vol. 139, no. 1, pp. 199–210, 2009.
- [7] K. Miyazaki, M. Mesaki, and N. Ishida, "Nuclear entry mechanism of rat PER2 (rPER2): role of rPER2 in nuclear localization of CRY protein.," *Mol. Cell. Biol.*, vol. 21, pp. 6651–9, Oct. 2001.
- [8] C. H. Ko and J. S. Takahashi, "Molecular components of the mammalian circadian clock.," *Hum. Mol. Genet.*, vol. 15, pp. R271–7, Oct. 2006.
- [9] K. Kume, M. J. Zylka, S. Sriram, L. P. Shearman, D. R. Weaver, X. Jin, E. S. Maywood, M. H. Hastings, and S. M. Reppert, "mCRY1 and mCRY2 are essential components of the negative limb of the circadian clock feedback loop," *Cell*, vol. 98, no. 2, pp. 193–205, 1999.

## Bibliography

---

- [10] J.-C. Leloup and A. Goldbeter, "Toward a detailed computational model for the mammalian circadian clock," *Proc. Natl. Acad. Sci. U. S. A.*, vol. 100, pp. 7051–6, June 2003.
- [11] H. P. Mirsky, A. C. Liu, D. K. Welsh, S. A. Kay, and F. J. Doyle, "A model of the cell-autonomous mammalian circadian clock," *Proc. Natl. Acad. Sci. U. S. A.*, vol. 106, pp. 11107–12, July 2009.
- [12] D. B. Forger and C. S. Peskin, "A detailed predictive model of the mammalian circadian clock," *Proc. Natl. Acad. Sci. U. S. A.*, vol. 100, pp. 14806–11, Dec. 2003.
- [13] C. Lee, J.-P. Etchegaray, F. R. Cagampang, A. S. I. Loudon, and S. M. Reppert, "Posttranslational mechanisms regulate the mammalian circadian clock," *Cell*, vol. 107, pp. 855–67, Dec. 2001.
- [14] Y. Lee, R. Chen, H.-m. Lee, and C. Lee, "Stoichiometric relationship among clock proteins determines robustness of circadian rhythms," *J. Biol. Chem.*, vol. 286, pp. 7033–42, Mar. 2011.
- [15] N. A. Cookson, L. S. Tsimring, and J. Hasty, "The pedestrian watchmaker: genetic clocks from engineered oscillators," *FEBS Lett.*, vol. 583, pp. 3931–7, Dec. 2009.
- [16] N. Kurabayashi, T. Hirota, M. Sakai, K. Sanada, and Y. Fukada, "DYRK1A and glycogen synthase kinase 3beta, a dual-kinase mechanism directing proteasomal degradation of CRY2 for circadian timekeeping," *Mol. Cell. Biol.*, vol. 30, pp. 1757–68, Apr. 2010.
- [17] E. Vielhaber, E. Eide, A. Rivers, Z.-H. Gao, and D. M. Virshup, "Nuclear Entry of the Circadian Regulator mPER1 Is Controlled by Mammalian Casein Kinase Ie," *Mol. Cell. Biol.*, vol. 20, pp. 4888–4899, July 2000.
- [18] E. A. Griffin Jr., D. Staknis, and C. J. Weitz, "Light-Independent Role of CRY1 and CRY2 in the Mammalian Circadian Clock," *Science*, vol. 286, pp. 768–771, Oct. 1999.
- [19] J. Andersson, B. Houska, and M. Diehl, "Towards a Computer Algebra System with Automatic Differentiation for use with Object-Oriented modelling languages," *3rd Int. Work. Equation-Based Object-Oriented Model. Lang. Tools*, pp. 99–105, 2010.
- [20] A. C. Hindmarsh, P. N. Brown, K. E. Grant, S. L. Lee, R. Serban, D. A. N. E. Shumaker, and C. S. Woodward, "SUNDIALS : Suite of Nonlinear and Differential / Algebraic Equation Solvers," *ACM Trans. Math. Softw.*, vol. 31, no. 3, pp. 363–396, 2005.
- [21] A. K. Wilkins, B. Tidor, J. White, and P. I. Barton, "Sensitivity Analysis for Oscillating Dynamical Systems," *SIAM J. Sci. Comput.*, vol. 31, no. 4, p. 2706, 2009.

- [22] A. Relógio, P. O. Westermark, T. Wallach, K. Schellenberg, A. Kramer, and H. Herz, "Tuning the Mammalian Circadian Clock: Robust Synergy of Two Loops," *PLoS Comput. Biol.*, vol. 7, p. e1002309, Dec. 2011.
- [23] A. C. Liu, D. K. Welsh, C. H. Ko, H. G. Tran, E. E. Zhang, A. A. Priest, E. D. Buhr, O. Singer, K. Meeker, I. M. Verma, F. J. Doyle, J. S. Takahashi, and S. A. Kay, "Intercellular coupling confers robustness against mutations in the SCN circadian clock network," *Cell*, vol. 129, pp. 605–16, May 2007.
- [24] R. N. Gutenkunst, J. J. Waterfall, F. P. Casey, K. S. Brown, C. R. Myers, and J. P. Sethna, "Universally sloppy parameter sensitivities in systems biology models," *PLoS Comput. Biol.*, vol. 3, pp. 1871–78, Oct. 2007.
- [25] D. B. Kell and J. D. Knowles, "The role of modeling in systems biology," in *Syst. Model. Cell. Biol. from concepts to nuts bolts* (Z. Szallasi, J. Stelling, and V. Periwal, eds.), pp. 3–18, Cambridge: MIT Press, 2006.
- [26] A. Raue, C. Kreutz, T. Maiwald, J. Bachmann, M. Schilling, U. Klingmüller, and J. Timmer, "Structural and practical identifiability analysis of partially observed dynamical models by exploiting the profile likelihood," *Bioinformatics*, vol. 25, pp. 1923–9, Aug. 2009.
- [27] M. Nihtilä and J. Virkkunen, "Practical identifiability of growth and substrate consumption models," *Biotechnol. Bioeng.*, vol. 19, pp. 1831–50, Dec. 1977.
- [28] J. E. Jiménez-Hornero, I. M. Santos-Dueñas, and I. García-García, "Optimization of biotechnological processes. The acetic acid fermentation. Part II: Practical identifiability analysis and parameter estimation," *Biochem. Eng. J.*, vol. 45, pp. 7–21, June 2009.
- [29] A. Holmberg, "On the practical identifiability of microbial growth models incorporating Michaelis-Menten type nonlinearities," *Math. Biosci.*, vol. 62, pp. 23–43, Nov. 1982.
- [30] M. Joshi, A. Seidel-Morgenstern, and A. Kremling, "Exploiting the bootstrap method for quantifying parameter confidence intervals in dynamical systems," *Metab. Eng.*, vol. 8, pp. 447–55, Sept. 2006.
- [31] M. E. Hughes, L. DiTacchio, K. R. Hayes, C. Vollmers, S. Pulivarthy, J. E. Baggs, S. Panda, and J. B. Hogenesch, "Harmonics of circadian gene transcription in mammals," *PLoS Genet.*, vol. 5, p. e1000442, Apr. 2009.
- [32] T. Hirota, J. W. Lee, W. G. Lewis, E. E. Zhang, G. Breton, X. Liu, M. Garcia, E. C. Peters, J.-P. Etchegaray, D. Traver, P. G. Schultz, and S. A. Kay, "High-Throughput Chemical Screen Identifies a Novel Potent Modulator of Cellular Circadian Rhythms and Reveals CKI $\alpha$  as a Clock Regulatory Kinase," *PLoS Biol.*, vol. 8, p. e1000559, Dec. 2010.

- [33] T. Hirota, W. G. Lewis, A. C. Liu, J. W. Lee, P. G. Schultz, and S. A. Kay, "A chemical biology approach reveals period shortening of the mammalian circadian clock by specific inhibition of GSK-3beta.," *Proc. Natl. Acad. Sci. U. S. A.*, vol. 105, pp. 20746–51, Dec. 2008.
- [34] L. T. Biegler, *Nonlinear Programming: Concepts, Algorithms, and Applications to Chemical Processes*. SIAM, 2010.
- [35] H. G. Bock, E. Kostina, and J. P. Schloder, "Numerical methods for parameter estimation in nonlinear differential algebraic equations," *GAMM Mitteilungen*, vol. 408, no. 2, pp. 376 – 408, 2007.
- [36] C. A. Floudas, *Nonlinear and Mixed-Integer Optimization*. New York, New York, USA: Oxford University Press, 1995.
- [37] A. Wachter and L. T. Biegler, "On the implementation of an interior-point filter line-search algorithm for large-scale nonlinear programming," *Math. Program.*, vol. 106, pp. 25–57, Apr. 2006.
- [38] HSL, "A collection of Fortran codes for large scale scientific computation," 2011.
- [39] J. Andersson, *A General-Purpose Software Framework for Dynamic Optimization*. Phd thesis, Arenberg Doctoral School, KU Leuven, Department of Electrical Engineering (ESAT/SCD) and Optimization in Engineering Center, Kasteelpark Arenberg 10, 3001-Heverlee, Belgium, Oct. 2013.
- [40] E. Jones, T. Oliphant, and P. Peterson, "SciPy: Open Source Scientific Tools for Python," 2001.
- [41] R. Serban and A. C. Hindmarsh, "CVODES: the Sensitivity-Enabled ODE Solver in SUNDIALS," in *Proc. IDETC/CIE 2005*, (Long Beach, CA), 2005.
- [42] M. A. Kramer, H. Rabitz, and J. M. Calo, "Sensitivity analysis of oscillatory systems," *Appl. Math. Model.*, vol. 8, pp. 328–340, Oct. 1984.
- [43] E. G. Bure and E. Rosenwasser, "The study of the sensitivity of oscillatory systems," *Autom. Remote Control*, vol. 7, pp. 1045–1052, 1974.
- [44] D. E. Zak, G. E. Gonye, J. S. Schwaber, and F. J. Doyle, "Importance of input perturbations and stochastic gene expression in the reverse engineering of genetic regulatory networks: insights from an identifiability analysis of an in silico network.," *Genome Res.*, vol. 13, pp. 2396–405, Nov. 2003.
- [45] J. Bass, "Circadian topology of metabolism.," *Nature*, vol. 491, pp. 348–56, Nov. 2012.
- [46] R. Ye, C. P. Selby, N. Ozturk, Y. Annayev, and A. Sancar, "Biochemical analysis of the canonical model for the mammalian circadian clock.," *J. Biol. Chem.*, vol. 286, pp. 25891–902, July 2011.

- [47] K. Yagita, F. Tamanini, M. Yasuda, J. H. J. Hoeijmakers, G. T. J. van der Horst, and H. Okamura, "Nucleocytoplasmic shuttling and mCRY-dependent inhibition of ubiquitylation of the mPER2 clock protein.," *EMBO J.*, vol. 21, pp. 1301–14, Mar. 2002.
- [48] J. S. Takahashi, H.-K. Hong, C. H. Ko, and E. L. McDearmon, "The genetics of mammalian circadian order and disorder: implications for physiology and disease.," *Nat. Rev. Genet.*, vol. 9, pp. 764–75, Oct. 2008.
- [49] S. Reischl, K. Vanselow, P. I. O. Westermark, N. Thierfelder, B. Maier, H. Herz, and A. Kramer, "Beta-TrCP1-mediated degradation of PERIOD2 is essential for circadian dynamics.," *J. Biol. Rhythms*, vol. 22, pp. 375–86, Oct. 2007.
- [50] A. Takano, Y. Isojima, and K. Nagai, "Identification of mPer1 phosphorylation sites responsible for the nuclear entry.," *J. Biol. Chem.*, vol. 279, pp. 32578–85, July 2004.
- [51] L. Busino, F. Bassermann, A. Maiolica, C. Lee, P. M. Nolan, S. I. H. Godinho, G. F. Draetta, and M. Pagano, "SCFFbxl3 controls the oscillation of the circadian clock by directing the degradation of cryptochrome proteins.," *Science*, vol. 316, pp. 900–4, May 2007.
- [52] S. I. H. Godinho, E. S. Maywood, L. Shaw, V. Tucci, A. R. Barnard, L. Busino, M. Pagano, R. Kendall, M. M. Quwailid, M. R. Romero, J. O'neill, J. E. Chesham, D. Brooker, Z. Lalanne, M. H. Hastings, and P. M. Nolan, "The after-hours mutant reveals a role for Fbxl3 in determining mammalian circadian period.," *Science*, vol. 316, pp. 897–900, May 2007.
- [53] S. M. Siepka, S.-H. Yoo, J. Park, W. Song, V. Kumar, Y. Hu, C. Lee, and J. S. Takahashi, "Circadian mutant Overtime reveals F-box protein FBXL3 regulation of cryptochrome and period gene expression.," *Cell*, vol. 129, pp. 1011–23, June 2007.
- [54] Y. Lee and E.-K. Kim, "AMP-activated protein kinase as a key molecular link between metabolism and clockwork.," *Exp. Mol. Med.*, vol. 45, p. e33, Jan. 2013.
- [55] M. Gallego, E. J. Eide, M. F. Woolf, D. M. Virshup, and D. B. Forger, "An opposite role for tau in circadian rhythms revealed by mathematical modeling.," *Proc. Natl. Acad. Sci. U. S. A.*, vol. 103, pp. 10618–23, July 2006.
- [56] E. S. Maywood, J. E. Chesham, Q.-J. Meng, P. M. Nolan, A. S. I. Loudon, and M. H. Hastings, "Tuning the period of the mammalian circadian clock: additive and independent effects of CK1 $\epsilon$ Tau and Fbxl3Afh mutations on mouse circadian behavior and molecular pacemaking.," *J. Neurosci.*, vol. 31, pp. 1539–44, Jan. 2011.
- [57] K. Vanselow, J. T. Vanselow, P. I. O. Westermark, S. Reischl, B. Maier, T. Korte, A. Herrmann, H. Herz, A. Schlosser, and A. Kramer, "Differential effects of

## Bibliography

---

- PER2 phosphorylation: molecular basis for the human familial advanced sleep phase syndrome (FASPS)," *Genes Dev.*, vol. 20, pp. 2660–72, Oct. 2006.
- [58] P. C. St. John and F. J. Doyle, "Estimating confidence intervals in predicted responses for oscillatory biological models," *BMC Syst. Biol.*, vol. 7, p. 71, July 2013.
- [59] R. Gunawan and F. J. Doyle, "Isochron-based phase response analysis of circadian rhythms," *Biophys. J.*, vol. 91, pp. 2131–41, Sept. 2006.
- [60] K. Ohsaki, K. Oishi, Y. Kozono, K. Nakayama, K. I. Nakayama, and N. Ishida, "The role of beta-TrCP1 and beta-TrCP2 in circadian rhythm generation by mediating degradation of clock protein PER2," *J. Biochem.*, vol. 144, pp. 609–18, Nov. 2008.
- [61] H. Lee, R. Chen, Y. Lee, S. Yoo, and C. Lee, "Essential roles of CKIdelta and CKIepsilon in the mammalian circadian clock," *Proc. Natl. Acad. Sci. U. S. A.*, vol. 106, pp. 21359–64, Dec. 2009.